A Study of MHD Couple Stress Casson Fluid Flow Over A Stretching Sheet with Hall Effects

Thesis Submitted In Partial Fulfillment of the Requirements for the Award of Degree of
Masters of Science
in
Mathematics & Computing

Submitted by
Cheenu Bansal
Roll No.: 301603005

Under the Guidance of
Dr. Raj Nandkeolyar
Assistant Professor

School of Mathematics
THAPAR INSTITUTE OF ENGINEERING & TECHNOLOGY
PATIALA - 147004, INDIA

June, 2018

Certificate

I hereby certify that the work which is being presented in the thesis entitled "**A Study of MHD Couple Stress Casson Fluid Flow Over A Stretching Sheet with Hall Effects**" in partial fulfillment of the requirements for the award of degree of Master of Science in "Mathematics and Computing" at the School of Mathematics, Thapar Institute of Engineering and Technology, Patiala is an authentic record of my own work studied under the supervision of Dr. Raj Nandkeolyar.

The matter embodied in this thesis has not been submitted by me for the award of any other degree of this or any other University/Institute.

Cheenu Bansal
(Roll No. 301603005)

This is to certify that the above statement made by the candidate is correct and true to the best of my knowledge.

Dr. Raj Nandkeolyar
Assistant Professor,
School of Mathematics,
Thapar Institute of Engineering and Technology, Patiala

Acknowledgements

I find no words to express my indebtedness to my thesis supervisor, Dr. Raj Nandkeolyar, Assistant Professor, Thapar Institute of Engineering & Technology, Patiala, for his valuable guidance and support throughout my work. I thank him for his constant encouragement and advice he has provided throughout my time as his student.

I would like to express my deep sense of gratitude to Dr. Satish Kumar Sharma, Head (School of Mathematics), and Dr. A.K.Lal, Associate Professor (School of Mathematics) Thapar Institute of Engineering & Technology Patiala, for providing the necessary facilities needed to carry out the results. I would also like to thank the faculty members and administrative staff of School of Mathematics, Thapar Institute of Engineering & Technology, Patiala who have contributed directly or indirectly to this work.

Its been a great time at Thapar Institute of Engineering & Technology, Patiala with friends who have been always there for me, listening to me, rejoicing me, complaining and pondering my way throughout my study and decisions in life. I would thank them for their great company.

Last but not the least, I would like to thank my parents for their continuous support which inspired me and encouraged me, without them I would not have been able to complete this work.

Abstract

The thesis is divided into four chapters in which Chapter-1 is introductory, which presents some basic terminology and history of the research in fluid mechanics. Chapter-2 presents a theoretical study of the unsteady three dimensional flow of a couple stress Casson over a linearly stretching sheet under the effects of Hall current, radiative heat transfer, and Newtonian heating at the surface of the sheet. In Chapter-3, the work presented in Chapter-2 is extended to consider the effects of nanoparticles by including the effects of thermopherosis and Brownian diffusion. Lastly, in Chapter-4, the significant findings of the thesis and the scope for future work is presented.

Chapter 1 is the introductory which presents a brief history of fluid dynamics along with an outline of the most important contributions made by several researchers on the topics of fluid dynamics. This chapter then presents a short account on the various types of fluids, types of fluid flow, the magnetohydrodynamics (MHD) phenomena, and the Hall effects with its applications. The main idea of this chapter is to introduce some of the basic terms used in the later parts of the thesis.

Chapter-2 theoretically investigates the unsteady three dimensional flow of a couple stress Casson fluid over a linearly stretching sheet in the presence of an externally applied magnetic field. The effects of Hall current and radiative heat transfer is taken into account while the effect of induced magnetic field is neglected. The surface of the sheet is assumed to be heated via a Newtonian heating process by some external means. The fluid flow phenomena is modelled in terms of nonlinear partial differential equations along with suitable boundary conditions. A set of similarity transformations were then utilized to obtain nonlinear ordinary differential equations from the governing partial differential equations, which were then solved by a spectral method based quasilinearization technique, known as, spectral quasilinearization technique (SQLM). Important results concerning the fluid flow, heat and mass transfer, as well as, related to skin-friction, heat and mass transfer coefficients, were obtained in the form of graphs and table.

The effects of presence of nanoparticles in the base fluid on the fluid flow problem considered in Chapter-2 is presented Chapter-3. Thus, Chapter-3 is devoted to study the transient hydromagnetic three dimensional flow of a couple stress Casson nanofluid over a linearly stretching sheet including the effects of Hall current and radiative heat transfer. The fluid flow model considered in this chapter incorporates the effect of the thermopherosis and Brownian diffusion which arise due to the presence of nanoparticles in the base fluid. The solution process is same as adopted in Chapter-2 and the results are discussed with the help of graphs and tables.

Contents

Certificate **i**

Acknowledgements **ii**

Abstract **iii**

List of Figures **vi**

List of Tables **viii**

1 Basics of Fluid Dynamics **1**
1.1 Introduction 1
1.2 History 1
1.3 Types of Fluids 4
1.3.1 Viscous (or real) and Inviscid (or perfect or ideal) Fluids 4
1.3.2 Newtonian and Non-Newtonian Fluids 4
1.3.2.1 Casson Fluid 5
1.3.3 Incompressible and Compressible fluids 5
1.4 Types of Flows 5
1.4.1 Steady and Unsteady Flow 5
1.4.2 Uniform and Non Uniform Flow 6
1.4.3 Laminar and Turbulent Flow 6
1.4.4 Irrotational and Rotational Flow 7
1.5 Couple Stress in Fluids 7
1.6 Magnetohydrodynamic Phenomenon 7
1.7 Hall Current 8

2 Unsteady Three-Dimensional Couple Stress Casson Fluid Flow with Thermal Radiation and Hall Effects **9**
2.1 Abstract 9
2.2 Introduction 9
2.3 Mathematical Formulation 11
2.4 Numerical Solution 14
2.5 Results and Discussions 16

3 Unsteady Three-Dimensional Couple Stress Casson Nanofluid Flow with Thermal Radiation and Hall Effects **32**
3.1 Abstract 32
3.2 Introduction 32
3.3 Mathematical Formulation 33
3.4 Numerical Solution 36
3.5 Results and Conclusions 39

4 Conclusions and Future Scope **59**
4.1 Conclusions drawn from Chapters 59
4.2 Scope for Future Research 60

Bibliography **61**

List of Figures

2.1 Effect of Casson parameter β on (a) f', (b) h when $A = 0.1,\ K = 1.5,\ M = 0.5,\ m = 0.1,\ Pr = 7,\ N = 1,\ Sc = 2$ 19
2.2 Effect of Casson parameter β on (a) θ, (b) ϕ when $A = 0.1,\ K = 1.5,\ M = 0.5,\ m = 0.1,\ Pr = 7,\ N = 1,\ Sc = 2$ 20
2.3 Effect of A on (a) f', (b) h when $\beta = 0.5,\ K = 1.5,\ M = 0.5,\ m = 0.1,\ Pr = 7,\ N = 1,\ Sc = 2$ 21
2.4 Effect of A on (a) θ, (b) ϕ when $\beta = 0.5,\ K = 1.5,\ M = 0.5,\ m = 0.1,\ Pr = 7,\ N = 1,\ Sc = 2$ 22
2.5 Effect of Couple stress parameter(K) on (a) f', (b) h when $\beta = 0.5,\ A = 0.1,\ M = 0.5,\ m = 0.1,\ Pr = 7,\ N = 1,\ Sc = 2$ 23
2.6 Effect of Couple stress parameter(K) on (a) θ, (b) ϕ when $\beta = 0.5,\ A = 0.1,\ M = 0.5,\ m = 0.1,\ Pr = 7,\ N = 1,\ Sc = 2$ 24
2.7 Effect of Magnetic parameter(M) on (a) f', (b) h when $\beta = 0.5,\ K = 1.5,\ A = 0.1,\ m = 0.1,\ P = 7,\ N = 1,\ Sc = 2$ 25
2.8 Effect of Magnetic parameter(M) on (a) θ, (b) ϕ when $\beta = 0.5,\ K = 1.5,\ A = 0.1,\ m = 0.1,\ P = 7,\ N = 1,\ Sc = 2$ 26
2.9 Effect of Hall current(m) on (a) f', (b) h, when $\beta = 0.5,\ K = 1.5,\ M = 0.5,\ A = 0.1,\ P = 7,\ N = 1,\ Sc = 2$ 27
2.10 Effect of Hall current(m) on (a) θ, (b) ϕ when $\beta = 0.5,\ K = 1.5,\ M = 0.5,\ A = 0.1,\ P = 7,\ N = 1,\ Sc = 2$ 28
2.11 Effect of Pr on (a) θ when $\beta = 0.5,\ K = 1.5,\ M = 0.5,\ m = 0.1,\ A = 0.1,\ N = 1,\ Sc = 2$ 29
2.12 Effect of Conduction Radiation parameter(N) on (a) θ, when $\beta = 0.5,\ K = 1.5,\ M = 0.5,\ m = 0.1,\ Pr = 7,\ A = 0.1,\ Sc = 2$ 29
2.13 Effect of Sc on ϕ when $\beta = 0.5,\ K = 1.5,\ M = 0.5,\ m = 0.1,\ Pr = 7,\ N = 1,\ A = 0.1$ 30

3.1 Effect of Couple stress parameter(K) on (a) f', (b) h when $\beta = 0.1,\ A = 0.01,\ M = 5,\ m = 0.1,\ Pr = 3,\ N = 1,\ N_t = 0.1,\ N_b = 0.1,\ Le = 5$ 42
3.2 Effect of Couple stress parameter(K) on (a) θ, (b) ϕ when $\beta = 0.1,\ A = 0.01,\ M = 5,\ m = 0.1,\ Pr = 3,\ N = 1,\ N_t = 0.1,\ N_b = 0.1,\ Le = 5$ 43
3.3 Effect of Casson Fluid Parameter (β) on (a) f', (b) h when $K = 0.5,\ A = 0.01,\ M = 5,\ m = 0.1,\ Pr = 3,\ N = 1,\ N_t = 0.1,\ N_b = 0.1,\ Le = 5$ 44
3.4 Effect of Casson Fluid Parameter (β) on (a) θ, (b) ϕ when $K = 0.5,\ A = 0.01,\ M = 5,\ m = 0.1,\ Pr = 3,\ N = 1,\ N_t = 0.1,\ N_b = 0.1,\ Le = 5$ 45
3.5 Effect of A on (a) f', (b) h when $\beta = 0.1,\ K = 0.5,\ M = 5,\ m = 0.1,\ Pr = 3,\ N = 1,\ N_t = 0.1,\ N_b = 0.1,\ Le = 5$ 46
3.6 Effect of A on (a) θ, (b) ϕ when $\beta = 0.1,\ K = 0.5,\ M = 5,\ m = 0.1,\ Pr = 3,\ N = 1,\ N_t = 0.1,\ N_b = 0.1,\ Le = 5$ 47

3.7 Effect of Magnetic Radiation (M) on (a) f', (b) h when $\beta = 0.1,\ A = 0.01,\ K = 0.5,\ m = 0.1,\ Pr = 3,\ N = 1,\ N_t = 0.1,\ N_b = 0.1,\ Le = 5$ . . . 48
3.8 Effect of Magnetic Radiation (M) on (a) θ, (b) ϕ when $\beta = 0.1,\ A = 0.01,\ K = 0.5,\ m = 0.1,\ Pr = 3,\ N = 1,\ N_t = 0.1,\ N_b = 0.1,\ Le = 5$ . . . 49
3.9 Effect of Hall Current Effect (m) on (a) f', (b) h when $\beta = 0.1,\ A = 0.01,\ M = 5,\ K = 0.5,\ Pr = 3,\ N = 1,\ N_t = 0.1,\ N_b = 0.1,\ Le = 5$ 50
3.10 Effect of Hall Current Effect (m) on (a) θ, (b) ϕ when $\beta = 0.1,\ A = 0.01,\ M = 5,\ K = 0.5,\ Pr = 3,\ N = 1,\ N_t = 0.1,\ N_b = 0.1,\ Le = 5$ 51
3.11 Effect of Pr on (a) θ, (b) ϕ when $\beta = 0.1,\ A = 0.01,\ M = 5,\ m = 0.1,\ K = 0.5,\ N = 1,\ N_t = 0.1,\ N_b = 0.1,\ Le = 5$ 52
3.12 Effect of N on θ, when $\beta = 0.1,\ A = 0.01,\ M = 5,\ m = 0.1,\ Pr = 3,\ K = 0.5,\ N_t = 0.1,\ N_b = 0.1,\ Le = 5$ 53
3.13 Effect of N_t on (a) θ, (b) ϕ when $\beta = 0.1,\ A = 0.01,\ M = 5,\ m = 0.1,\ Pr = 3,\ N = 1,\ K = 0.5,\ N_b = 0.1,\ Le = 5$ 54
3.14 Effect of N_b on (a) θ, (b) ϕ when $\beta = 0.1,\ A = 0.01,\ M = 5,\ m = 0.1,\ Pr = 3,\ N = 1,\ N_t = 0.1,\ K = 0.5,\ Le = 5$ 55
3.15 Effect of Le on (a) θ, (b) ϕ when $\beta = 0.1,\ A = 0.01,\ M = 5,\ m = 0.1,\ Pr = 3,\ N = 1,\ N_t = 0.1,\ N_b = 0.1,\ K = 0.5$ 56

List of Tables

1.1 Classification of fluids on the basis of density and viscosity: 5

2.1 Numerical Values for different physical parameters: 31

3.1 Numerical Values for different physical parameters: 57
3.2 Numerical Values for different physical parameters: 58

Dedicated to My Parents

Chapter 1

Basics of Fluid Dynamics

1.1 Introduction

A fluid is anything that flows, usually a liquid or a gas. The relative compressibilities differentiates the liquids and gases from each other. Fluid dynamics or Hydrodynamics is that branch of science which is concerned with the study of the motion of fluids or that of bodies in contact with fluids. The viscosity and vorticity, formalism of continuum mechanics, energy and momentum in a fluid, the conservation of mass, the Euler and Navier-Stokes equations are the key concepts used in Fluid dynamics.
Applications in fluid dynamics are:

1. Potential flow around a cylinder.
2. The Stokes flow, the propagation of sound and gravity waves and many more.

1.2 History

The history of fluid dynamics includes the most important contributions of a number of scientists and engineers. It can be said that already at the beginning of the nineteenth century the basic equations with which fluid flows can be described reliably were known. Solutions of these equations were not possible owing to the lack of suitable solution methods for engineering problems and therefore technical hydraulics developed alongside the field of theoretical fluid dynamics. For geometrically complicated problems, methods based on similarity laws were used to generalize experimentally achieved flow results. Analytical methods only allowed the solution of academic problems that had no relevance for practical applications. It was not until the second half of the twentieth

century that the development of suitable methods led to the numerical techniques that we have today which allow us to solve the basic equations of fluid dynamics for practically relevant flow problems. Parallel to the development of the numerical methods, the development of experimental techniques was also pushed ahead, so that nowadays measurement techniques are available which allow us to obtain experimentally fluid dynamics data that are interesting for practical flow problems. Contributions made by few notable researchers are presented below:

- **Archimedes (287 BC-212 BC)** formulated the laws of buoyancy which are applied to floating and submerged bodies. This later on forms the differential calculus as part of the analysis.
- **Ab u Rayhan Al-Biruni (973-1048)** was the first to apply experimental scientific methods to fluid statics. For instance, determining the specific weights. The correlation between the specific gravity of an object and the volume of water it displaces was discovered by Biruni.
- **Leonardo da Vinci (1452-1519)** derived the equation of conservation of mass in one-dimensional steady flow. His works includes the accurate descriptions of jets, waves, hydraulic pumps and both low-drags (streamlined) and high-drag (parachute) designs.
- **Evangelista Torricelli (1608-1647)** invented the mercurial barometer. It was discovered from solving an important practical problem. This was the first barometer. This discovery has perpetuated his fame. Torr, which is a unit of pressure, was named after his name. It is commonly used in vacuum measurements. and Chantilly. He built the first wind tunnel and tested models in it.
- **Blaise Pascal (1623-1662)** presented the study of hydrodynamics and hydrostatics centered on the principles of hydraulic fluids. He invented the hydraulic press and the syringe. He generalized the work of Evangelista Torricelli by clarifying the concepts of pressure and vacuum. He also made important contributions to the study of fluids.
- **Isaac Newton (1642-1727)** postulated his laws of motion and the law of viscosity of the linear fluids now called Newtonian fluid.
- **Daniel Bernoulli (1700-1782)** and Euler together tried to discover more about the flow of fluids. The relationship between the speed at which blood flows and its pressure was found by them. The air speed in modern aircrafts is measured by Bernoulli's method.

- **Leonhard Euler (1707-1783)** introduced the Bernoulli equation which is also known as differential equations of motion of fluids and their integral form. This calculus has the application to the motion of water by d'Alembert, and enabled both d'Alembert and Euler to represent the theory of fluids in formulae restricted by no particular hypothesis.

- **Jean le Rond d'Alembert (1717-1783)** the famous paradox: that a body immersed in a frictionless fluid has zero drag was invented by him using the Euler's equation.

- **Antoine Chzy (1718-1798)** was the first to express the mean flow velocity in terms of channel roughness, hydraulic radius, and bed slope. This formula describes the mean flow velocity of steady, turbulent open channel flow $\nu = C\sqrt{Ri}$.

- **Pierre Louis Georges Dubuat (1734-1809)** was one of the most successful worker of his period in the field of hydrodynamics. He published a revised edition of his Principes d'hydraulique in 1786. This book includes a satisfactory theory of the motion of fluids. This book is based on the experiments made by himself.

- **St. Venant (1797-1886)** formulated the equations of unsteady flow in open channels.

- **Poiseuille (1797-1869)** derived experimentally in 1838, and in 1840 and 1846 formulated and published, Poiseuille's law. This concerns the voluminal laminar stationary flow of an incompressible uniform viscous liquid (so-called Newtonian fluid) through a cylindrical tube with constant circular cross-section.

- **Gaspard Riche de Prony (17551839)**: The theory of running water was greatly advanced by the researches he had done. He also discovered the simple expression for running water's velocity.

- **Johann Albert Eytelwein (1764-1848)** had made theories about effect of water on the velocities of stream. He proved that when the circumference of wheel was considered half of the velocity of stream, then water wheel shows its maximum effect.

- **Jean Nicolas Pierre Hachette (1769-1834)** published memoirs containing the results of experiments on the spouting of fluids and the discharge of vessels in 1816-1817.

- **Osborne Reynolds (1842-1912)** published the classic pipe experiment in 1883. In the honor of his work, the dimensionless Reynolds number was named after him.

- **Navier (1785-1836) and Stokes (1819-1903)** derived the Navier-Stokes which govern the motion of fluids. These equations are made using the Newton's second law to fluid motion. It is also assumed that the the sum of a diffusing viscous term and a pressure term is fluid stress.
  Applications:

  1. The equations are extremely useful because they describe the physics of many things of academic and economic interest.
  2. They may be used to model the weather, water flow in a pipe, air flow around a wing.

- **Ludwig Prandtl (1875-1953)** pointed out that fluid flows with small viscosity (water and air flows) can be divided into following categories:
  a thin viscous layer,
  or boundary layer,
  near solid surfaces and interfaces,
  patched onto a nearly inviscid outer layer, where the Euler and Bernoulli equations apply.

1.3 Types of Fluids

1.3.1 Viscous (or real) and Inviscid (or perfect or ideal) Fluids

A fluid is said to be *viscous* when normal as well as shearing stresses exist. On the other hand, a fluid is said to be *inviscid* when it doesn't exert any shearing stress, whether at rest or in motion. Clearly the pressure exerted by a inviscid fluid on any surface is always normal to the surface at that point.

1.3.2 Newtonian and Non-Newtonian Fluids

The fluid that satisfies the Newton's Law of Viscosity i.e.,

$$\tau = \mu \frac{du}{dy},$$

is called Newtonian fluid, otherwise the fluid is an example of Non-Newtonian fluid. Non-Newtonian fluid are toothpaste, ketchup, custard, honey etc. One of such Non-Newtonian fluid is **Casson fluid**.

TABLE 1.1: Classification of fluids on the basis of density and viscosity:

S.No.	Type of fluid	Density	Viscosity
1	Ideal fluid	constant	zero
2	Incompressible fluid	constant	zero or non-zero
3	Inviscid fluid	constant or variable	zero
4	Real fluid	Variable	non-zero
5	Newtonian fluid	constant or variable	non-zero and $\tau = \mu\frac{du}{dy}$
6	Non-Newtonian fluid	constant or variable	$\tau \neq \mu\frac{du}{dy}$
7	Compressible fluid	variable	zero or non-zero

1.3.2.1 Casson Fluid

Casson fluid is a shear thinning liquid which is assumed to have an infinite viscosity at zero rate of shear, and a zero viscosity at an infinite rate of shear. It behaves like elastic solids. The examples of Casson fluid are jelly, tomato sauce, honey, soup and concentrated fruit juices.
The application area of Casson fluid is to investigate the flow of blood (which is treated as Casson fluid) through a narrow artery with bell shaped stenosis.

1.3.3 Incompressible and Compressible fluids

Gases are compressible and their density changes readily with temperature and pressure. Liquids, on the other hand, are rather difficult to compress and for most problems we can treat them incompressible.

1.4 Types of Flows

The flow may be steady or unsteady, uniform or non-uniform, depending on the variation of flow and characterstics with time and space. The following is a characterization of types of fluid flow:

1.4.1 Steady and Unsteady Flow

If the fluid and flow characterstics such as density, velocity, pressure, accerelation etc, at a point do not change with time, the flow is said to be steady flow, thus for steady flow

$$\left(\frac{\partial p}{\partial t}\right)_{x_0,y_0,z_0} = 0,$$

$$\left(\frac{\partial v}{\partial t}\right)_{x_0,y_0,z_0} = 0,$$

and

$$\left(\frac{\partial \rho}{\partial t}\right)_{x_0,y_0,z_0} = 0,$$

In the unsteady flow one or more of the variables at a point may change with time. Thus,

$$\left(\frac{\partial p}{\partial t}\right)_{x_0,y_0,z_0} \neq 0,$$

$$\left(\frac{\partial v}{\partial t}\right)_{x_0,y_0,z_0} \neq 0,$$

and

$$\left(\frac{\partial \rho}{\partial t}\right)_{x_0,y_0,z_0} \neq 0,$$

Here (x_0, y_0, z_0) refers to a fixed point in the fluid, where these variables are being measured with respect to time.

1.4.2 Uniform and Non Uniform Flow

If the velocity vector at all the points in the flow is same (in magnitude as well as in direction) at any instant of time. the flow is said to be *uniform*. Thus,

$$\left(\frac{\partial v}{\partial s}\right)_{t_0} = 0,$$

in which ∂v is the change in velocity corresponding to a displacement ∂s in any direction s. Conversely the flow will be non uniform if the velocity vector varies from point to point at any instant of time, thus

$$\left(\frac{\partial v}{\partial s}\right)_{t_0} \neq 0.$$

1.4.3 Laminar and Turbulent Flow

In the laminar flow, the fluid particles move along smooth, regular paths which can be predicted well in advance. The particles thus move in laminas or layers gliding smoothly over the adjacent layers. The flow through a small diameter tube at a low velocity is

generally *laminar*. The *turbulent flow* is characterized by random and erratic movement of fluid particles resulting in formation of eddies. The eddy formation is responsible for high energy loss as compared to loss in laminar flow. The additional loss in turbulent flow is attributed to the existence of turbulent shear stress, which is many times larger than, laminar shear stress given by Newton's law of viscosity.

1.4.4 Irrotational and Rotational Flow

The concept of vorticity may be utilised for distinguishing as either irrotational or rotational. If the vorticity is zero at all the points in flow region, the flow in that region is known as *irrotational.* Thus, for irrotational flow, the vorticity is zero. In such flow zones, where the vorticity is non zero, the flow is said to be *rotational.* In actual flow problems, there may be zones possesing the characterstics of both rotational and irrotational flows.

1.5 Couple Stress in Fluids

The forces present in the fluid opposes the forces exerted by the additives mixed in the fluid, this opposite force is couple force and as a consequence the fluid is known as couple stress fluid.

1.6 Magnetohydrodynamic Phenomenon

The study of fluids that are electrically conducted is known as **Magnetohydrodynamics (MHD; also magneto-fluid dynamics)**. Examples of such fluids are liquid metals, salt water and plasmas. It is clear from the name that *magneto* means magnetic field, *hydro* means water and *dynamics* means movement.
The magnetic field can induce currents in moving conductive field, which makes fluid polarized and the fluid itself becomes magnetic field. The MHD equations are described from Navier-Stokes equations of fluid dynamics and Maxwell's equations of electromagnetism.

1.7 Hall Current

The production of a voltage difference across an electrical conductor is the Hall effect. The Hall effect is transverse to an electric current in the conductor. It is also transverse to an applied magnetic field perpendicular to the current. The Hall effect was discovered by **Edwin Hall** in 1879. Due to the nature of current in conductor the Hall effect arises. The movement of the many small charge carriers, typically electrons, holes, ions or all three constitute a current. These charges experience a force known as Lorentz force, when they comes in contact with magnetic field. Hall Current find appications in amny processes, such as in power sensing, to determine the type of semi-conductor, to determine the magnetic flux density etc.

Chapter 2

Unsteady Three-Dimensional Couple Stress Casson Fluid Flow with Thermal Radiation and Hall Effects

2.1 Abstract

This chapter theoretically investigates the unsteady three dimensional flow of a couple stress Casson fluid over a linearly stretching sheet in the presence of an externally applied magnetic field. The effects of Hall current and radiative heat transfer is taken into account while the effect of induced magnetic field is neglected. The surface of the sheet is assumed to be heated via a Newtonian heating process by some external means. A set of similarity transformations were then utilized to obtain nonlinear ordinary differential equations from the governing partial differential equations, which were then solved by a spectral method based quasilinearization technique, known as, spectral quasilinearization technique (SQLM). Important results were obtained in the form of graphs and table.

2.2 Introduction

The boundary layer flow over a stretching surface has relevance in many engineering processes. Sakiadis [1] for the very first time examined the boundary-layer behavior on continuous surfaces, moving continuous flat surfaces and moving continuous cylindrical

surfaces. This also includes the work of Crane [2]. He investigated the study of incompressible viscous fluid over an elastic sheet. These studies have the application in the polymer industry. For example, in a melt-spinning process, the extrudate is stretched into filament or sheet while it is drawn from the die. Carragher and Crane [3] and Gupta and Gupta [4] investigated the heat transfer of a flow in stretching surface maintained at constant and variable temperatures.

The magnetohydrodynamic (MHD) flows are of great importance in various industrial processes, such as purification of crude oil, paper production, glass manufacturing, geophysics. Due to these applications, Pavlov [5] investigated the effect of a magnetic field on the viscous flow of an electrically conducting fluid past a stretching sheet. The effect of the mass transfer corresponding to the similarity solution for the MHD flow over a stretching permeable surface subject to injection is studied by Pop and Na [6]. He investigated the results for the large values of mass transfer parameter. The analytical solution is discussed by Ellahi and Raiz [7] for the MHD flow in a third grade fluid with variable viscosity.

The industrial applications of non-Newtonian fluid flow are increasing day by day. The boundary-layer flows of non-Newtonian fluids due to a stretching plane were investigated by Rajagopal et. al [8]. Due to increasing importance of Non-Newtonian fluids in industrial processes, many research works had been made. One of such Non-Newtonian fluid is Casson fluid. Casson fluid is a shear thinning liquid which is assumed to have an infinite viscosity at zero rate of shear, and a zero viscosity at an infinite rate of shear (Dash et al. [9]). It behaves like elastic solids. The examples of Casson fluid are jelly, tomato sauce, honey, soup and concentrated fruit juices. The application area of Casson fluid is to investigate the flow of blood (which is treated as Casson fluid) through a narrow artery with bell shaped stenosis. Another investigation was done by Bird et al. [10]. He investigated the rheology and flow of visco-plastic materials. The steady flow of Casson fluid was investigated by Fredrickson [11]. Soret and Dufour effects on magnetohydrodynamic (MHD) flow of Casson fluid was investigated by Hayat et al. [12].

Because of the flow behaviour of the Non-Newtonian fluid cannot be predicted by Naviers-Stokes alone and also the tensor for couple stress fluid is not symmetric, therefore couple stress along with Non-Newtonian fluids are studied altogether. Couple stress fluids are the fluids that consists of rigid randomly oriented particles suspended in a viscous medium. Examples of such types of fluid are lubricants containing small amount of polymer additives, synthetic fluids, blood and many more. The thermal instability of a couple stress fluid with suspended particles, in the presence of rotation and magnetic field was investigated by Sharma and Sharma [13]. The incompressible laminar flow of a couple stress fluid in a porous channel with expanding or contracting walls was studied by Srinivasacharya et al. [14]. The study of combined effects of couple stresses and fluid inertia on the squeeze film characteristics between a long cylinder and an infinite plate

was done by Lin and Hung [15].

When the flow of viscous, incompressible electrically conducted fluid is subjected to voltage difference is produced across the conductivity fluid and transverse to the electric current in the conductor and applied magnetic field. This is known hall current and effect is known as Hall effect. The study of the Hall current and thermal radiation on the unsteady flow of viscous fluid over a permeable stretching surface was performed by Pal [16]. In his study, he observed that the magnetic parameter significantly affects the flow and the thermal fields, with the increasing range of buoyancy parameter. The heat and mass transfer with Joule heating on magnetohydrodynamic(MHD) peristaltic blood under the inuence of Hall effect was examined by Bhatti and Rashidi [17]. They observed that the Hall current and magnetic field show opposite behaviour on velocity and temperature profiles.

The studies mentioned above do not investigate the combined effects of couple stress, thermal radiation and unsteadiness on the three dimensional flow of a Casson fluid under the influence of an applied magnetic field and the resulting Hall current effects. The present chapter intends to present a numerical solution of the unsteady three dimensional MHD flow od a couple stress Casson fluid in the presence of Hall current, non-linear radiative heat transfer, convective heating and mass-transfer effects.

2.3 Mathematical Formulation

We consider the three dimensional unsteady flow of viscous incompressible couple stress Casson fluid over a surface $y = 0$. The fluid motion over the surface is caused due to a time dependent stretching of the surface in x-direction with velocity $u = U_w = \frac{ax}{1-ct}$. The fluid flow is permeated with a magnetic field $B(t)$ applied along the y-axis. The small magnetic Reynolds number assumption is taken into account to neglect the effects of induced magnetic field. However, the effects of Hall current on the flow field is retained. The surface of the sheet is heated by a hot fluid which causes a convective heat transfer with heat transfer coefficient h_s. Further, the concentration at the surface is denoted by C_f while, outside the boundary layer region, the concentration and temperature are C_∞ and T_∞ respectively.

Under the above assumptions, the equations governing the conservation of mass, momentum, energy and species concentration including the effects of Hall current, thermal radiation and couple stress, are

$$\frac{\partial u}{\partial x} + \frac{\partial v}{\partial y} + \frac{\partial w}{\partial z} = 0, \tag{2.1}$$

$$\frac{\partial u}{\partial t}+u\frac{\partial u}{\partial x}+v\frac{\partial u}{\partial y}+w\frac{\partial u}{\partial z}=\left(1+\frac{1}{\beta}\right)\nu\frac{\partial^2 u}{\partial y^2}-\nu'\frac{\partial^4 u}{\partial y^4}-\frac{\sigma B^2(t)}{\rho\,(1+m^2)}\,(u+mw)\,, \quad (2.2)$$

$$\frac{\partial w}{\partial t}+u\frac{\partial w}{\partial x}+v\frac{\partial w}{\partial y}+w\frac{\partial w}{\partial z}=\left(1+\frac{1}{\beta}\right)\nu\frac{\partial^2 w}{\partial y^2}-\nu'\frac{\partial^4 w}{\partial y^4}+\frac{\sigma B^2(t)}{\rho(1+m^2)}(mu-w), \quad (2.3)$$

$$\frac{\partial T}{\partial t}+u\frac{\partial T}{\partial x}+v\frac{\partial T}{\partial y}+w\frac{\partial T}{\partial z}=\frac{\partial}{\partial y}\left(\left(\alpha_m+\left(\frac{16\sigma^* T^3}{3\alpha^* C_p\rho}\right)\right)\frac{\partial T}{\partial y}\right), \quad (2.4)$$

$$\frac{\partial C}{\partial t}+u\frac{\partial C}{\partial x}+v\frac{\partial C}{\partial y}+w\frac{\partial C}{\partial z}=D\frac{\partial^2 C}{\partial y^2}. \quad (2.5)$$

.

The suitable boundary conditions are:

$u=u_w=\frac{ax}{1-ct}$, $v=0$, $w=0$, $\frac{\partial T}{\partial y}=-h_s T$, $C=C_f$, $\frac{\partial^2 u}{\partial y^2}\to 0$, $\frac{\partial^2 w}{\partial y^2}\to 0$ at $y=0$.

$u\to 0$, $w\to 0$, $T\to T_\infty$, $C\to C_\infty$, $\frac{\partial u}{\partial y}\to 0$, $\frac{\partial w}{\partial y}\to 0$, as $y\to\infty$.

where u, v and w are the velocities in x, y and z- directions respectively, $\nu=\frac{\mu}{\rho}$ is the kinematic viscocity, $\nu'=\frac{\eta}{\rho}$ is the couple stress viscosity, β is the Casson fluid parameter, ρ is the density, m is the Hall current, σ is the electric charge density, α_m is the thermal diffusivity, α^* is the Roseland mean absorption coefficient, σ^* is the Stefan-Boltzmann coefficient, h_s is the heat transfer coefficient, C_p is the specific heat capacity, C is the concentration of species, D is the coefficient of diffusing species, T_∞ and C_∞ are the ambient temperature and concentration respectively.

To obtain the similarity form of governing equations, we now use the transformations given by:

$u=\frac{ax}{(1-ct)}f'(\eta)$, $v=-\sqrt{\frac{a\nu}{(1-ct)}}f(\eta)$, $w=\frac{ax}{(1-ct)}h(\eta)$,

$\eta=y\sqrt{\frac{a}{\nu(1-ct)}}$, $\theta(\eta)=\frac{T-T_\infty}{T_\infty}$, $\phi(\eta)=\frac{C-C_\infty}{C_f-C_\infty}$.

Further, in order to get the true similarity solution, the time dependent transverse magnetic field is chosen as:

$$B^2(t)=\frac{(B_0)^2}{1-ct}$$

.

The governing differential equations after using the above transformations are:

$$\left(1+\frac{1}{\beta}\right)f'''-\left(f'^2-ff''\right)-A\left(\frac{\eta}{2}f''+f'\right)-Kf^v-\frac{M}{1+m^2}\left(f'+hm\right)=0, \tag{2.6}$$

$$\left(1+\frac{1}{\beta}\right)h''-\left(f'h-fh'\right)-A\left(\frac{\eta}{2}h'+h\right)-Kh^{iv}+\frac{M}{1+m^2}\left(f'm-h\right)=0, \tag{2.7}$$

$$\frac{1}{Pr}\theta''-\theta'\left(A\frac{\eta}{2}\right)+\theta' f+\frac{4}{3NPr}\left(\theta'(\theta+1)^3\right)'=0, \tag{2.8}$$

$$\frac{1}{Sc}\phi''-\phi'\left(A\frac{\eta}{2}-f\right). \tag{2.9}$$

The boundary conditions become:
At $y=0$

$$f=0, f'=1, h=0, \theta'=-\gamma\left(\theta+1\right), \phi=1, f'''=0, h''=0 \tag{2.10}$$

As $y\to\infty$

$$f'\to 0, h\to 0, f''\to 0, h'\to 0, \theta\to 0, \phi\to 0. \tag{2.11}$$

where, $a>0$ is the constant,

$A=\frac{c}{a}$ is the time dependent parameter,

$K=\frac{\nu' a}{\nu^2(1-ct)}$ is the couple stress parameter,

$M=\frac{\sigma(B_0)^2}{a\rho}$ is the magnetic parameter,

$Sc=\frac{\nu}{D}$ is the Schmidt number,

$Pr=\frac{\nu}{\alpha_m}$ is the Prandtl number,

$N=\frac{\rho\alpha^* C_p\alpha_m}{4\sigma^*(T_\infty)^3}$ is the conduction radiation parameter.

$\gamma=h_s\sqrt{\frac{\nu(1-ct)}{a}}$ is the conjugate parameter for Newtonian heating.

Skin friction along the x and z directions, Nusselt number and Sherwood number are given by:

$C_f Re_x^{\frac{1}{2}} = \left(1+\frac{1}{\beta}\right) f"(0) - Kf^v(0)$, $C_h Re_x^{\frac{1}{2}} = \left(1+\frac{1}{\beta}\right) h'(0) - Kh^{iv}(0)$,

$Nu_x Re_x^{-\frac{1}{2}} = \gamma\left(1+\frac{4(1+\theta(0))^3}{3N}\right)\left(1+\frac{1}{\theta(0)}\right)$, $ShRe_x^{-\frac{1}{2}} = -\phi'(0)$.

2.4 Numerical Solution

The numerical solution of the couple non-linear ordinary differential equations (2.6)-(2.9) subject to boundary conditions (2.10)-(2.11) is obtained by "Spectral Quasi Linearlisation Method". For this we assume,

$$L_1 = \left(1+\frac{1}{\beta}\right) f''' - \left(f'^2 - ff''\right) - A\left(\frac{\eta}{2}f'' + f'\right) - Kf^v - \frac{M}{1+m^2}\left(f' + hm\right),$$

$$L_2 = \left(1+\frac{1}{\beta}\right) h'' - \left(f'h - fh'\right) - A\left(\frac{\eta}{2}h' + h\right) - Kh^{iv} + \frac{M}{1+m^2}\left(f'm - h\right),$$

$$L_3 = \frac{1}{Pr}\theta'' - \theta'\left(A\frac{\eta}{2}\right) + \theta' f + \frac{4}{3NPr}\left(\theta'\left(\theta+1\right)^3\right)',$$

$$L_4 = \frac{1}{Sc}\phi'' - \phi'\left(A\frac{\eta}{2} - f\right),$$

The linear equation can be represented as

$$a_{11}^{(5)} f^v + a_{11}^{(4)} f^{iv} + a_{11}^{(3)} f''' + a_{11}^{(2)} f'' + a_{11}^{(1)} f' + a_{11}^{(0)} f + a_{12}^{(0)} h = R_1$$

where,

$$a_{11}^{(5)} = \frac{\partial L_1}{\partial f^v} = -K,$$

$$a_{11}^{(4)} = \frac{\partial L_1}{\partial f^{iv}} = 0,$$

$$a_{11}^{(3)} = \frac{\partial L_1}{\partial f^3} = \left(1+\frac{1}{\beta}\right),$$

$$a_{11}^{(2)} = \frac{\partial L_1}{\partial f^2} = f - \frac{A\eta}{2},$$

$$a_{11}^{(1)} = \frac{\partial L_1}{\partial f^1} = -2f'f'' - A - \frac{M}{1+m^2},$$

$$a_{11}^{(0)} = \frac{\partial L_1}{\partial f} = f'',$$

$$a_{12}^{(0)} = \frac{\partial L_1}{\partial h} = -\frac{Mm}{1+m^2},$$

$$R_1 = \sum_{i=0}^{5} \frac{\partial L_1}{\partial f^i} f^i + \sum_{i=0}^{5} \frac{\partial L_1}{\partial h^i} h^i - L_1 = ff'' + \left(f'\right)^2 - 2\left(f'\right)^2 f''.$$

The second linear equation for L_2 is as follows:

$$a_{22}^{(4)} h^{iv} + a_{22}^{(3)} h''' + ' + a_{22}^{(1)} h' + a_{22}^{(0)} h + a_{21}^{(1)} f' + a_{21}^{(0)} f = R_2$$

where,

$$a_{22}^{(4)} = \frac{\partial L_2}{\partial h^{iv}} = -K,$$

$$a_{22}^{(3)} = \frac{\partial L_2}{\partial h'''} = 0,$$

$$a_{22}^{(2)} = \frac{\partial L_2}{\partial h''} = \left(1 + \frac{1}{\beta}\right),$$

$$a_{22}^{(1)} = \frac{\partial L_2}{\partial h'} = f - \frac{A\eta}{2},$$

$$a_{22}^{(0)} = \frac{\partial L_2}{\partial h} = -f' - A - \frac{M}{1+m^2},$$

$$a_{21}^{(1)} = \frac{\partial L_2}{\partial f'} = -h + \frac{Mm}{1+m^2},$$

$$a_{21}^{(0)} = \frac{\partial L_2}{\partial f} = h',$$

$$R_2 = \sum_{i=0}^{5} \frac{\partial L_2}{\partial f^i} f^i + \sum_{i=0}^{5} \frac{\partial L_2}{\partial h^i} h^i - L_2 = -hf' + h'f.$$

Now, the third linear equation is represented as:

$$a_{33}^{(2)} \theta'' + a_{33}^{(1)} \theta' + a_{33}^{(0)} \theta + a_{31}^{(0)} f = R_3$$

where,

$$a_{33}^{(2)} = \frac{\partial L_3}{\partial \theta''} = \frac{1}{Pr} + \frac{4(\theta+1)^3}{3NPr},$$

$$a_{33}^{(1)} = \frac{\partial L_3}{\partial \theta'} = -\frac{A\eta}{2} + f + \frac{8(\theta+1)^2\theta'}{NPr},$$

$$a_{33}^{(0)} = \frac{\partial L_3}{\partial \theta} = \frac{4(\theta+1)\left((\theta+1)\theta'' + 2\theta'^2\right)}{NPr},$$

$$a_{31}^{(0)} = \frac{\partial L_3}{\partial f} = \theta',$$

$$R_3 = \frac{4\,(\theta+1)\left(\theta(\theta+1)\theta'' + (3\theta+1)(\theta')^2\right)}{NPr} + f\theta'.$$

Now the fourth linear equation can be represented as:

$$a_{44}^{(2)}\phi'' + a_{44}^{(1)}\phi' + a_{44}^{(0)}\phi + a_{41}^{(0)} f = R_4$$

where,

$$a_{44}^{(2)} = \frac{\partial L_4}{\partial \phi''} = \frac{1}{Sc},$$

$$a_{44}^{(1)} = \frac{\partial L_4}{\partial \phi'} = -\left(\frac{A\eta}{2} - f\right),$$

$$a_{44}^{(0)} = \frac{\partial L_4}{\partial \phi} = 0,$$

$$a_{41}^{(0)} = \frac{\partial L_4}{\partial f} = \phi',$$

$$R_4 = f\theta'.$$

2.5 Results and Discussions

The system of ordinary differential equations (2.6-2.9) is solved numerically using Spectral Quasi Linearlisation Method (SQLM) with MATLAB package. This shows the effect of velocity, temperature and concentration profiles on various parameters graphically. The results also have been discussed in tabulated form for more clear results. The default value is set for all dimensionless parameters. The default values set to record the results are Casson fluid parameter (β) = 0.5, Time dependent parameter (A) = 0.1, Couple stress parameter (K) = 1.5, Magnetic field parameter (M) = 0.5, Hall current effect (m) = 0.1, Prandtl number (Pr) = 7, Conduction radiation parameter (N) = 1, Schmidt number (Sc) = 2.

The influence of the Casson parameter can be seen in the fig(2.1-2.2). It depicts that there is a inverse relation between Casson fluid parameter and velocity profiles in x- and z-directions. When there is rise in Casson parameter, the velocity profiles show a declining behaviour, whereas in the fig(2.2(a) & (b)) there is a positive relation between the Casson parameter and temperature and concentration profiles. With the enhancement in Casson parameter, the concentration and temperature profile also enhances.

The effect of Couple stress parameter on velocity components in x- and z-directions, temperature and concentration profiles is portrait in fig(2.5-2.6). It is analyzed from the

fig(2.5(a) & (b)), that an increase in Time dependent parameter, the velocity profiles also show a positive result within a certain boundary. But after a certain boundary value the graphs shows the opposite results. This opposite result is due to the fact that the stretching coefficient is inversely proportion to the time dependent parameter. Fig(2.6) depicts that increase in time dependent parameter also increases the concentration and temperature profiles.

Fig(2.7-2.8) depicts the relation between velocity in x-, z-directions, temperature, concentration profiles and magnetic field parameter. It is observed that in fig(2.7(a)), velocity in x-direction decreases with the increase in magnetic field parameter. Fig(2.7(b)) shows that in a certain boundary the velocity in z-direction increases with the increase in magnetic field parameter followed by opposite relation between them. From the fig(2.8), it is cleared that increase in magnetic field parameter also enhances the temperature nd concentration boundary layers. This happens due to the presence of Lorentz force. It is force which is stronger corresponding to larger magnetic field parameter and also opposite to the fluid motion.

The variation of the velocity profiles with Hall parameter is shown in fig(2.9-2.10). The magnitudes of the velocity component u and the resultant velocity increase with the increase in Hall parameter throughout the channel. Also the concentration and temperature profiles in fig(2.10) shows the same relation as in velocity profiles.

The effect of Prandtl number on temperature profile can be seen in the fig(2.11). It is clearly evident from the fig that with the enhancement in Prandtl number, the graph of temperature falls. It is due to the fact that for higher values of Prandtl number, the thermal diffusivity decreases. As Prandtl number is the ratio of viscous diffusion rate and thermal diffusion rate.

The fig(2.12) shows the graphical relation between the conduction radiation parameter and temperature profiles. The fluid temperature decreases with the increase in conduction radiation parameter.

It is evident from the fig(2.13) that increase in Schmidt number the concentration profile shows a declining behaviour. The reason behind such a relation is that Schmidt number is inversely proportional to the diffusion coefficient. So, when Schmidt number is increased, concentration profile shows a declining effect.

The effect of the pertinent flow parameters such as the Casson parameter (β), unsteadiness parameter (A), couple stress parameter (K), magnetic parameter (M), Hall current parameter (m), Prandtl number (Pr), radiation parameter (N) and Schmidt number (Sc) on the skin-friction coefficients in x- and z- directions, Nusselt number and Sherwood number, wherever applicable are presented in Table 2.1. It is perceived from this table that the skin-friction coefficient increases with increasing couple stress and magnetic field in x-direction whereas decreases in z-direction. The skin-friction coefficient first decreases and then increases with the increasing transient nature. The skin-friction

coefficient in x-direction increases whereas in z-direction decreases with the increase in Hall current effect. An increase in Casson fluid parameter first decrease the skin-friction coefficient in x-direction and then increase it. Whereas it reduces the skin-friction coefficient in z-direction. The rate of heat transfer at the surface which is measured by $Nu_x Re_x^{\frac{-1}{2}}$ tend to get increased with the increase in couple stress, Hall effect, Prandtl number and thermal radiation whereas it decreases with the increase in Casson parameter and magnetic parameter. The unsteadiness parameter decreases with the increasing role of heat transfer. The effects of couple stress, Hall current and Schmidt number is to decrease the role of mass transfer at the surface, whereas the Casson parameter and magnetic parameter tend to enhance the mass transfer rate. The unsteadiness in the flow field increases with the increasing rate of mass transfer.

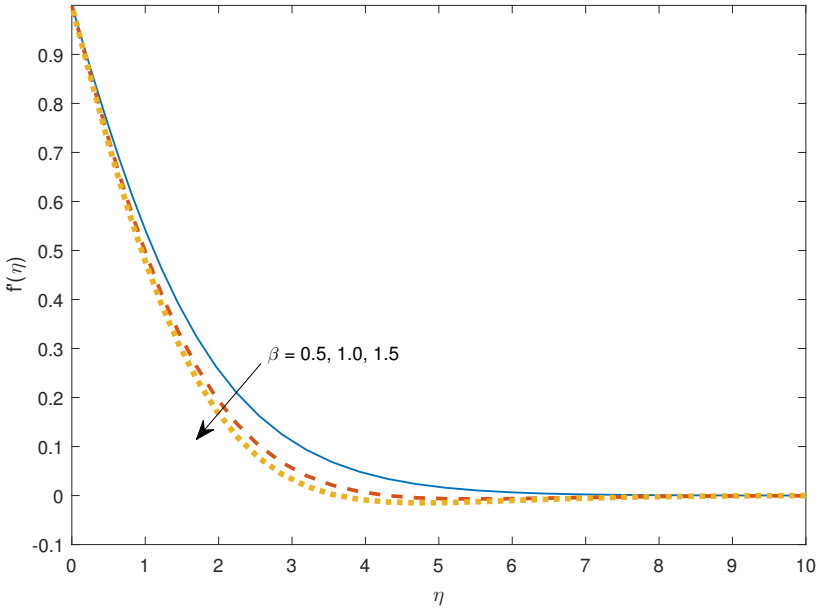

(a)

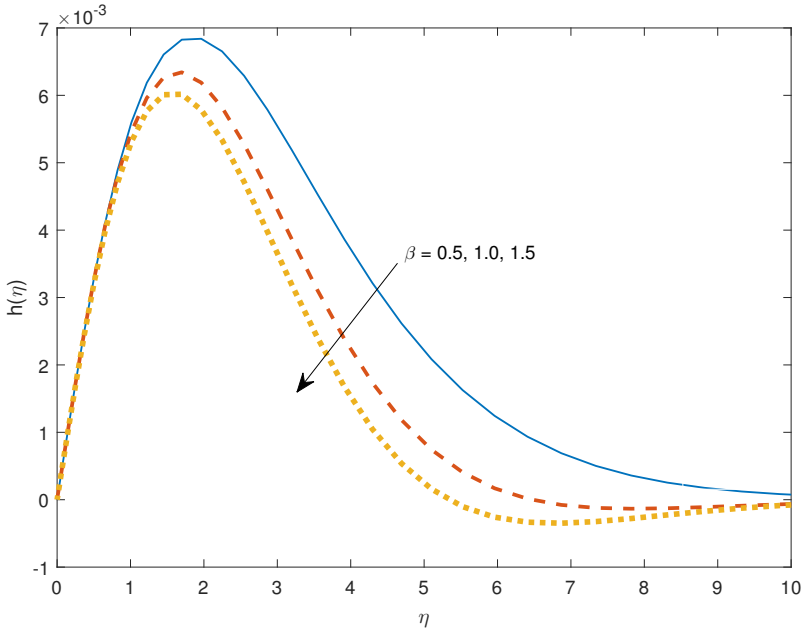

(b)

FIGURE 2.1: Effect of Casson parameter β on (a) f', (b) h when $A = 0.1$, $K = 1.5$, $M = 0.5$, $m = 0.1$, $Pr = 7$, $N = 1$, $Sc = 2$

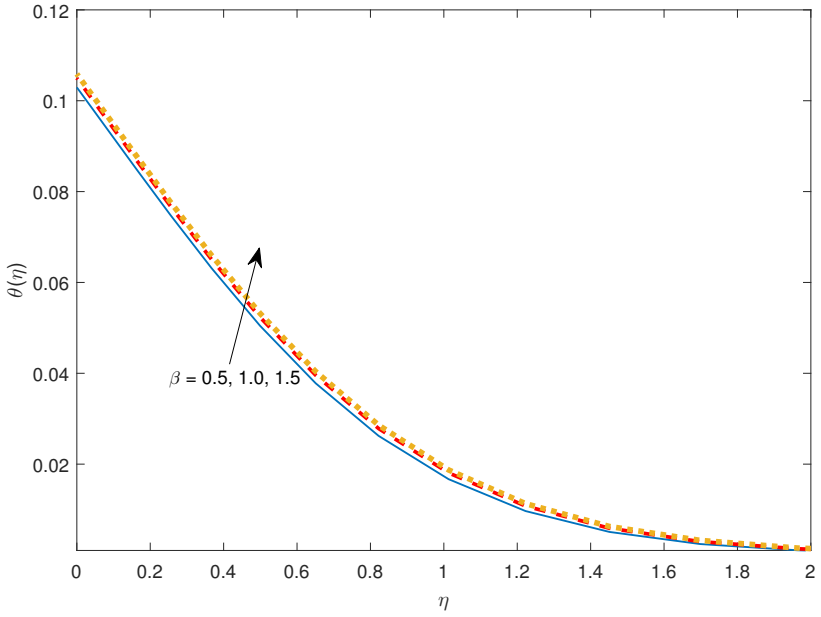

(a)

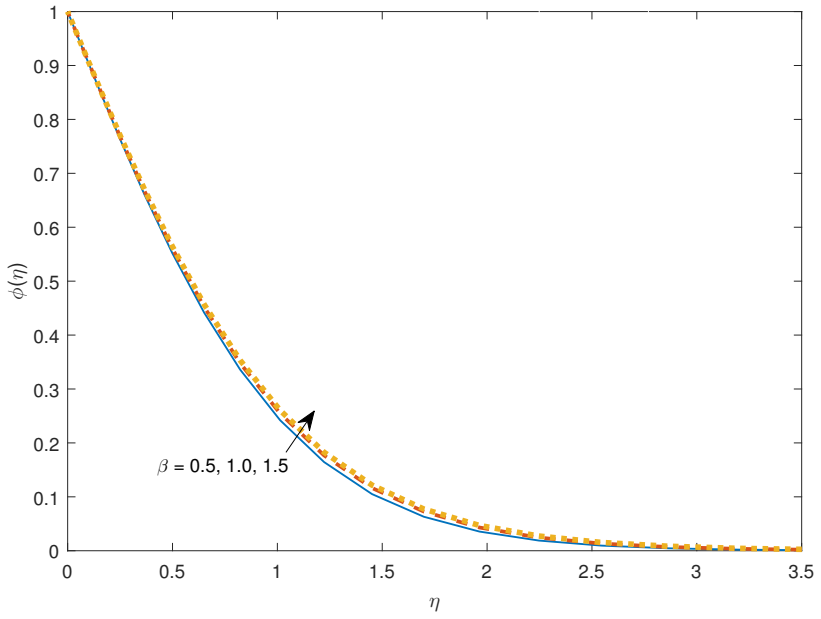

(b)

FIGURE 2.2: Effect of Casson parameter β on (a) θ, (b) ϕ when $A = 0.1,\ K = 1.5,\ M = 0.5,\ m = 0.1,\ Pr = 7,\ N = 1,\ Sc = 2$

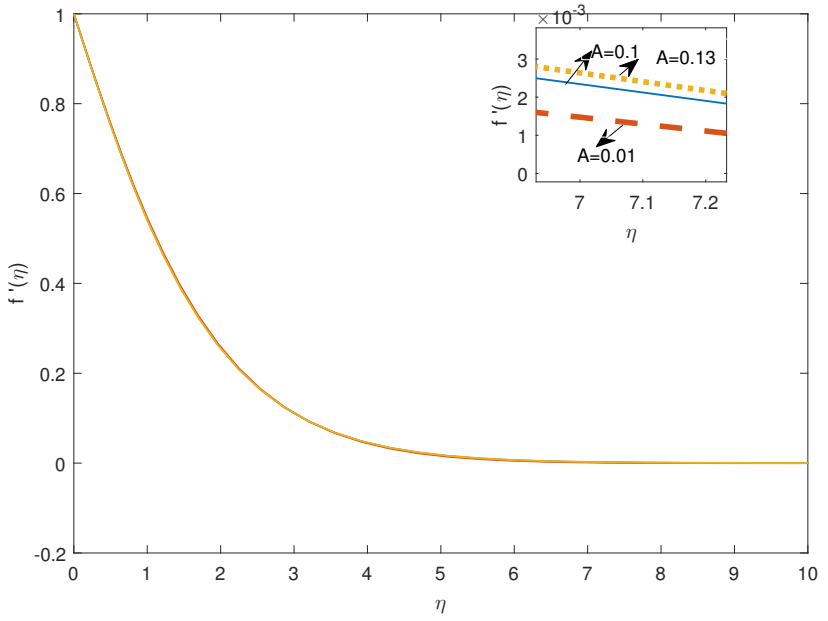

(a)

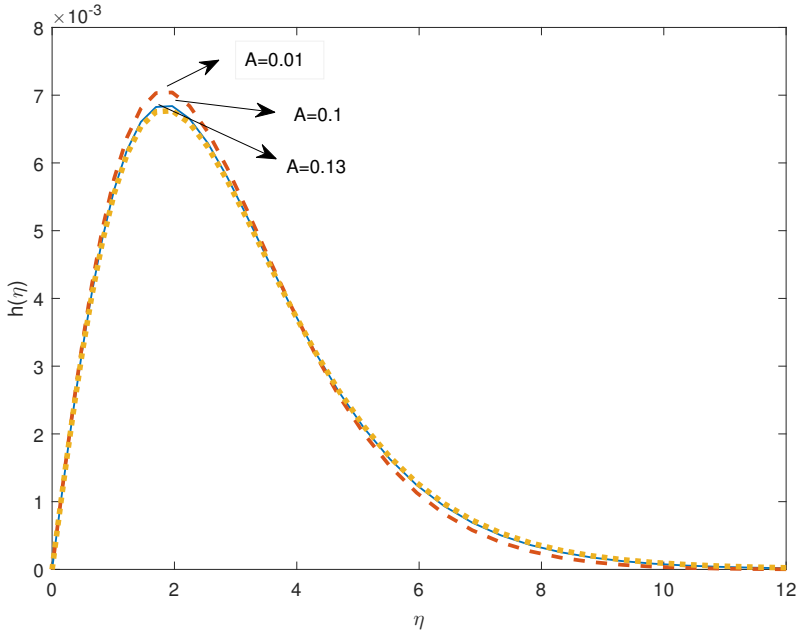

(b)

FIGURE 2.3: Effect of A on (a) f', (b) h when $\beta = 0.5,\ K = 1.5,\ M = 0.5,\ m = 0.1,\ Pr = 7,\ N = 1,\ Sc = 2$

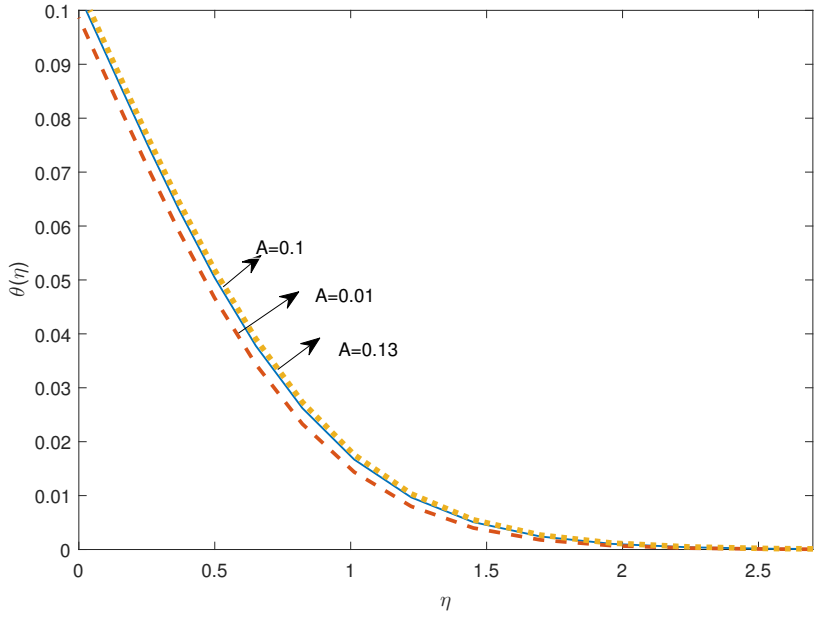

(a)

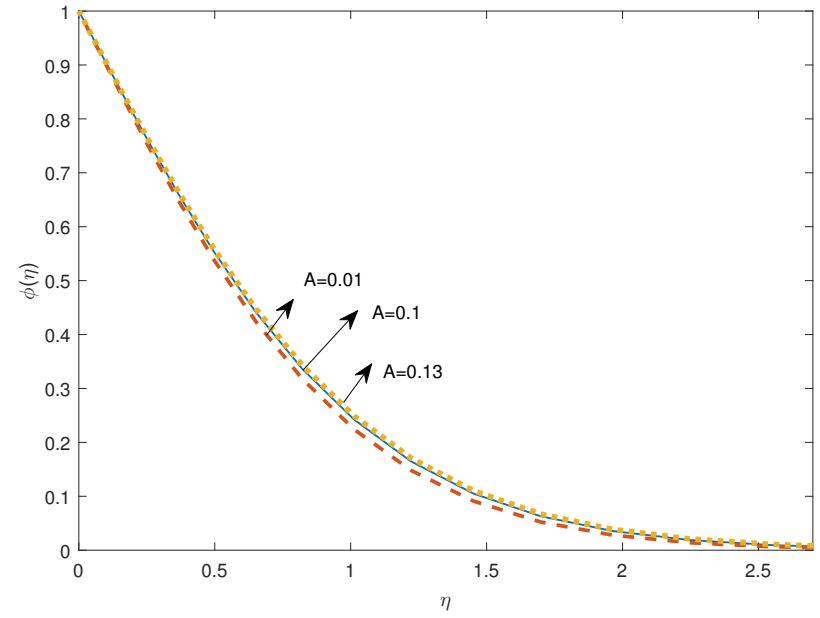

(b)

FIGURE 2.4: Effect of A on (a) θ, (b) ϕ when $\beta = 0.5,\ K = 1.5,\ M = 0.5,\ m = 0.1,\ Pr = 7,\ N = 1,\ Sc = 2$

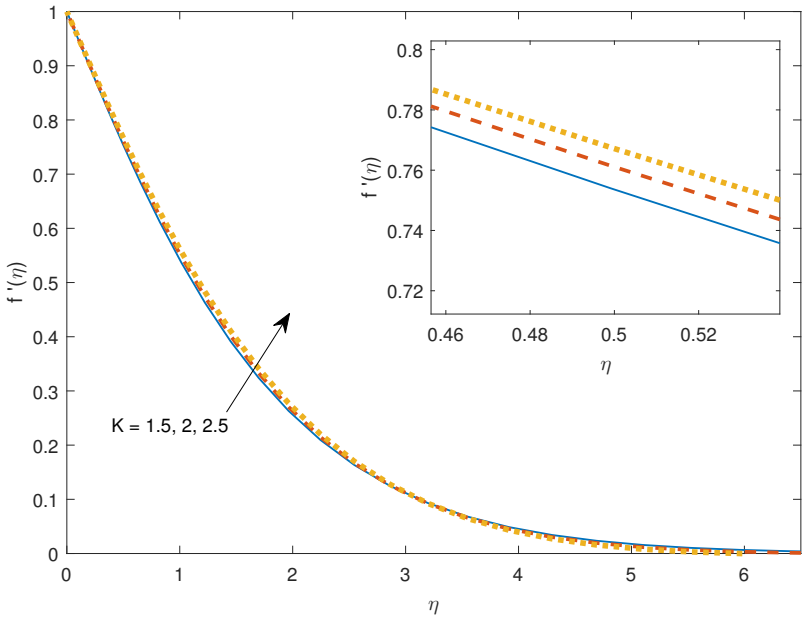

(a)

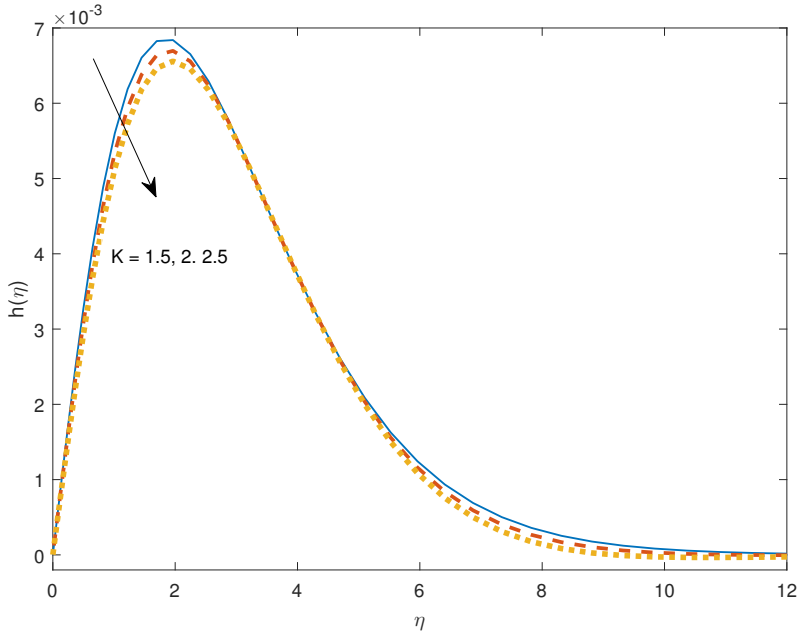

(b)

FIGURE 2.5: Effect of Couple stress parameter(K) on (a) f', (b) h when $\beta = 0.5,\ A = 0.1,\ M = 0.5,\ m = 0.1,\ Pr = 7,\ N = 1,\ Sc = 2$

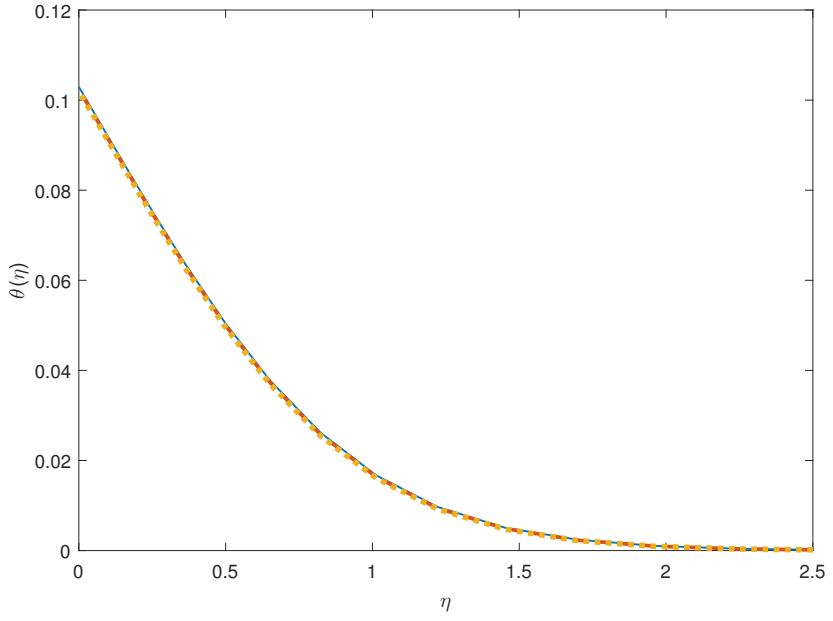

(a)

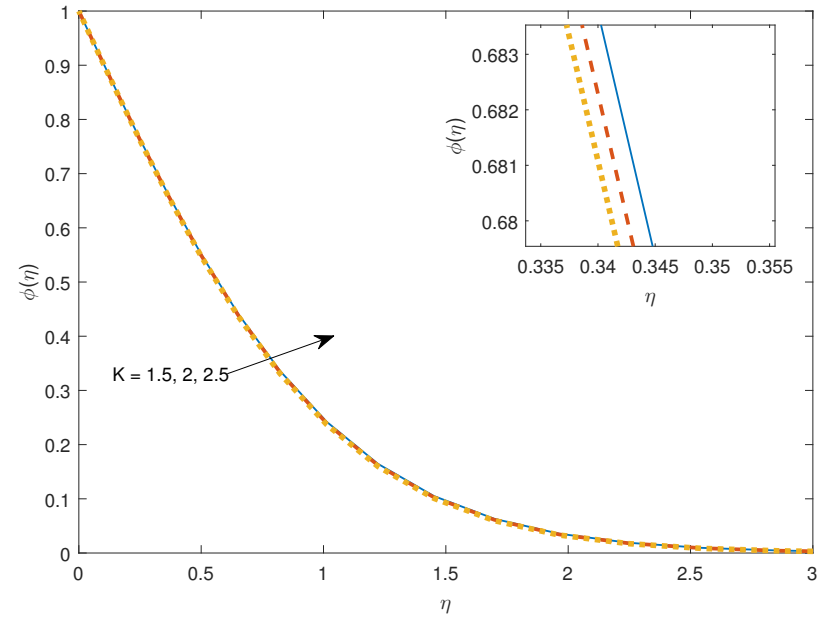

(b)

FIGURE 2.6: Effect of Couple stress parameter(K) on (a) θ, (b) ϕ when $\beta = 0.5,\ A = 0.1,\ M = 0.5,\ m = 0.1,\ Pr = 7,\ N = 1,\ Sc = 2$

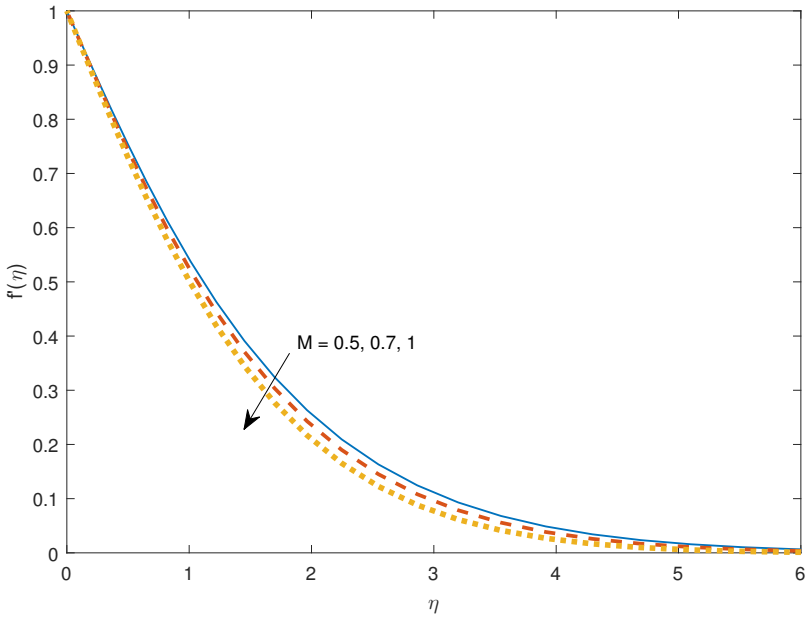

(a)

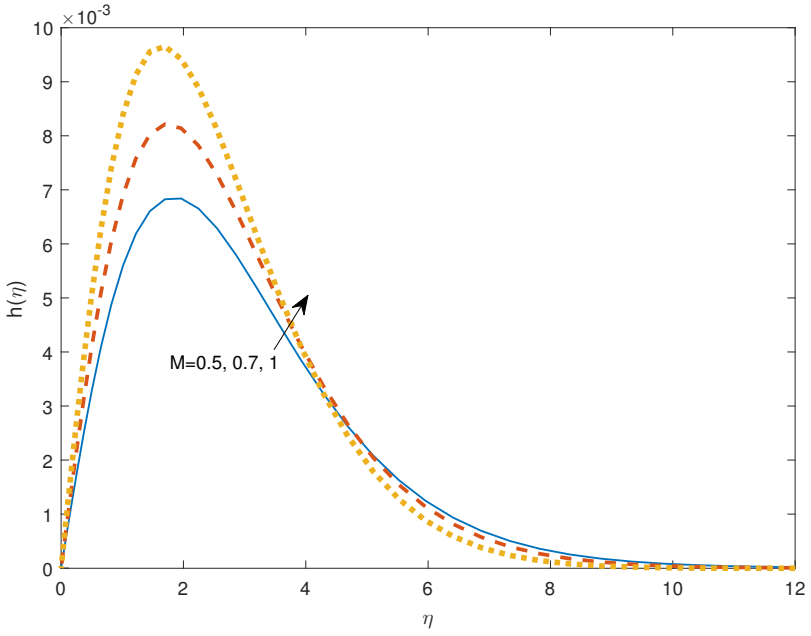

(b)

FIGURE 2.7: Effect of Magnetic parameter(M) on (a) f', (b) h when $\beta = 0.5,\ K = 1.5,\ A = 0.1,\ m = 0.1,\ P = 7,\ N = 1,\ Sc = 2$

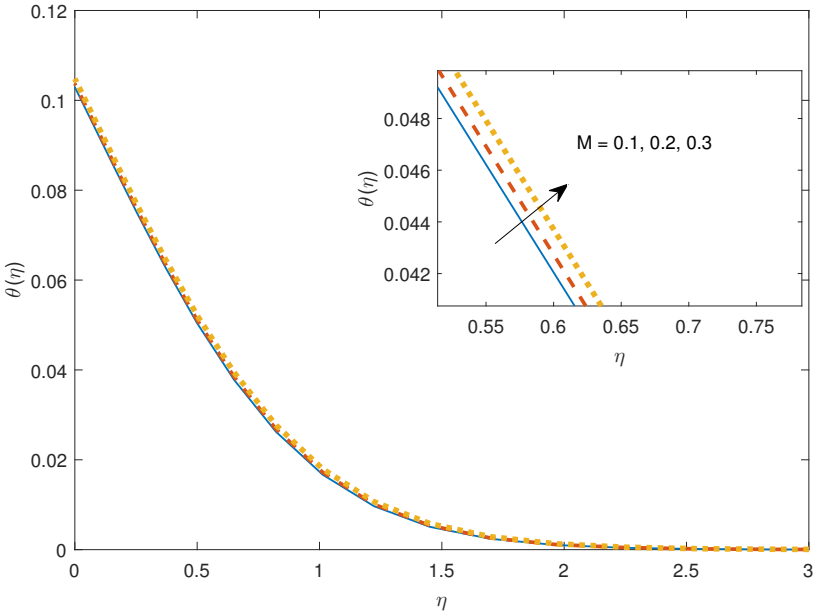

(a)

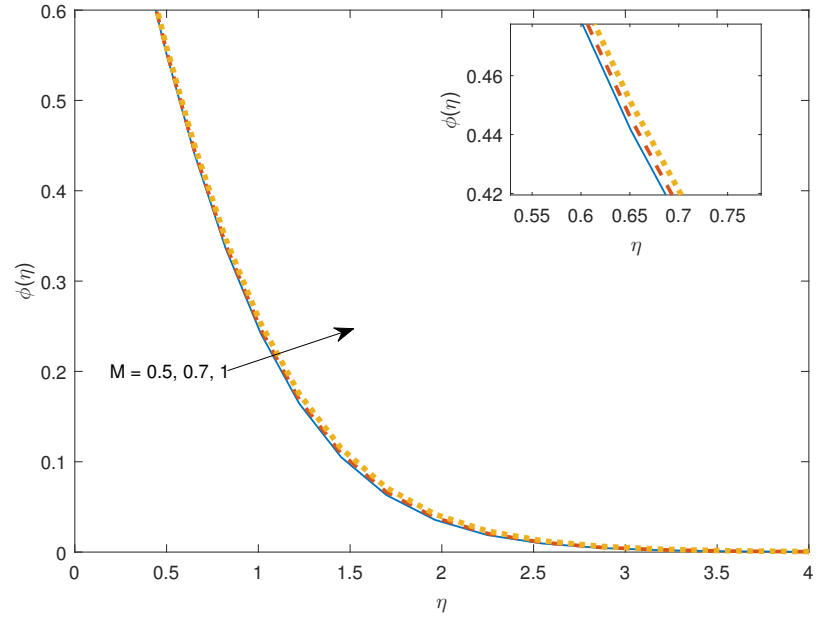

(b)

FIGURE 2.8: Effect of Magnetic parameter(M) on (a) θ, (b) ϕ when $\beta = 0.5,\ K = 1.5,\ A = 0.1,\ m = 0.1,\ P = 7,\ N = 1,\ Sc = 2$

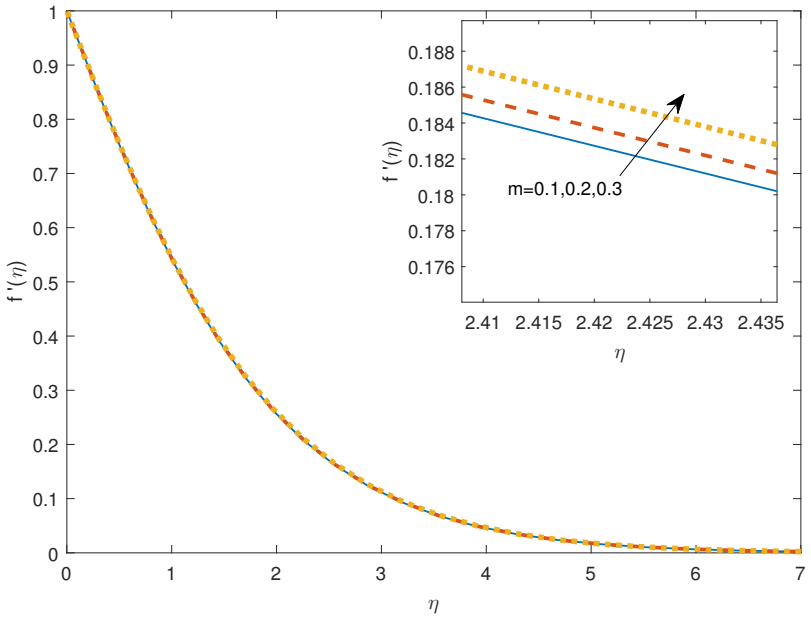

(a)

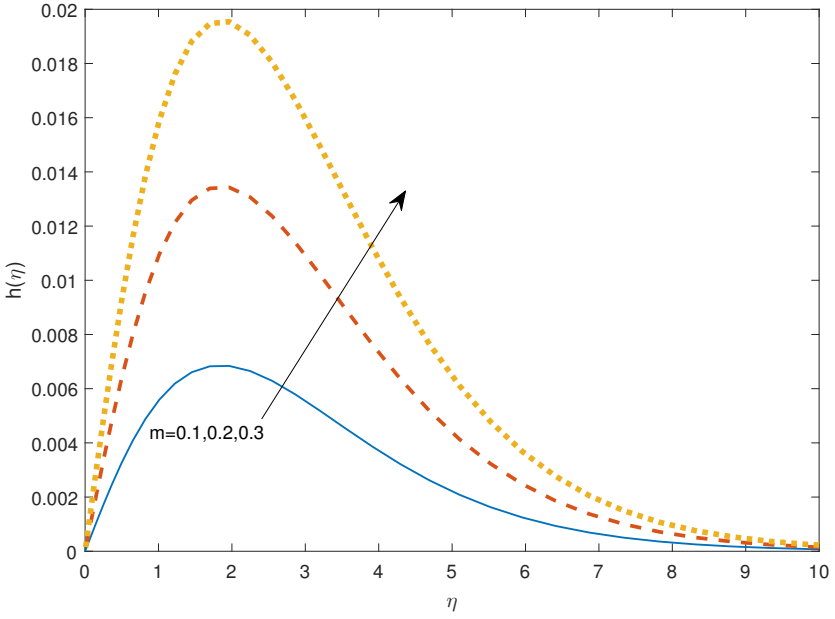

(b)

FIGURE 2.9: Effect of Hall current(m) on (a) f', (b) h, when $\beta = 0.5,\ K = 1.5,\ M = 0.5,\ A = 0.1,\ P = 7,\ N = 1,\ Sc = 2$

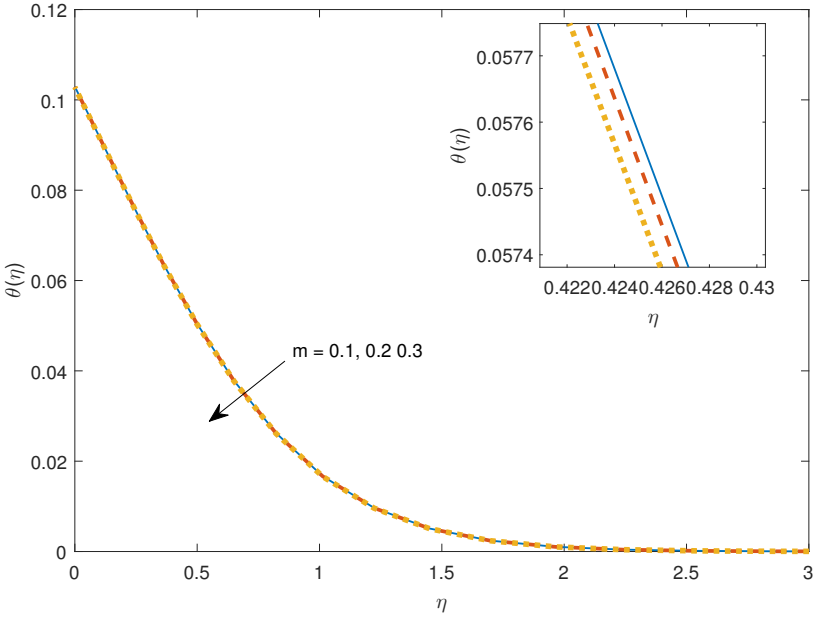

(a)

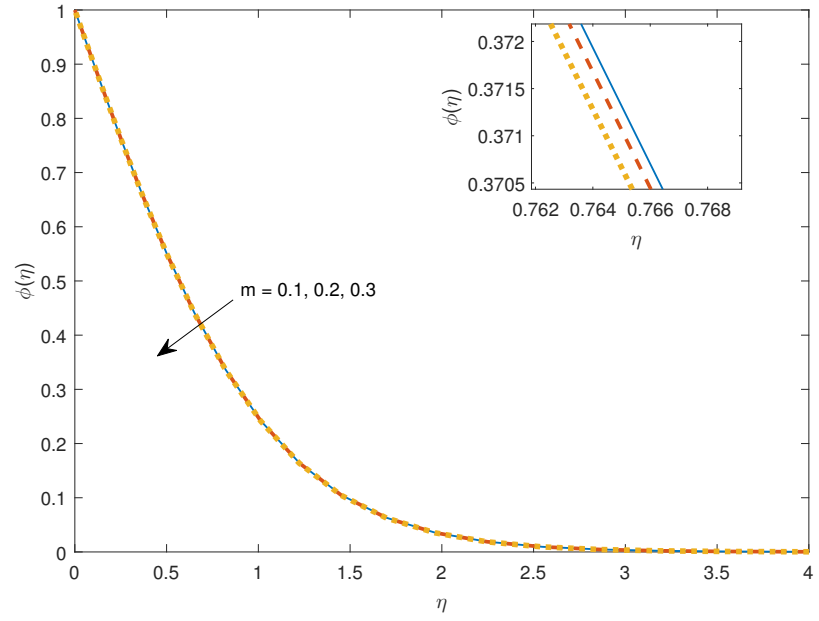

(b)

FIGURE 2.10: Effect of Hall current(m) on (a) θ, (b) ϕ when $\beta = 0.5,\ K = 1.5,\ M = 0.5,\ A = 0.1,\ P = 7,\ N = 1,\ Sc = 2$

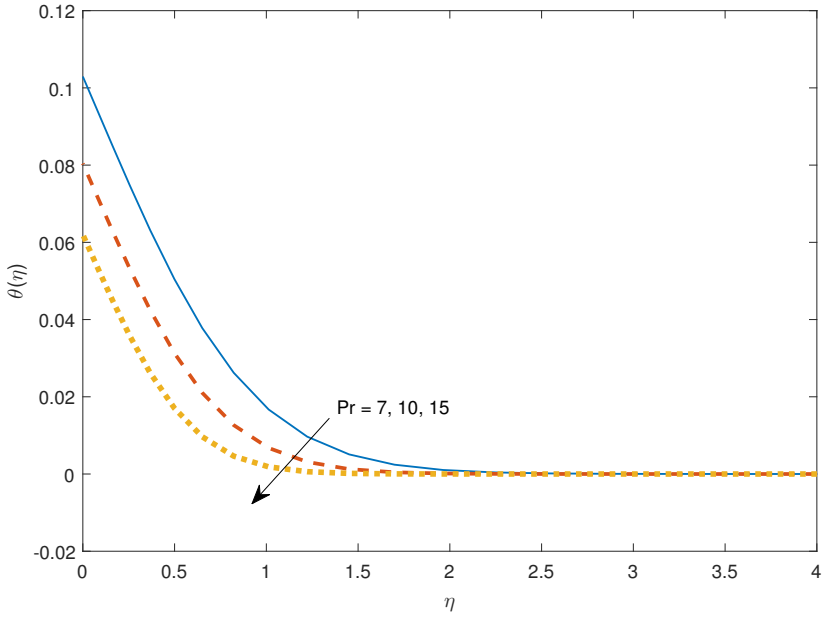

(a)

FIGURE 2.11: Effect of Pr on (a) θ when $\beta = 0.5,\ K = 1.5,\ M = 0.5,\ m = 0.1,\ A = 0.1,\ N = 1,\ Sc = 2$

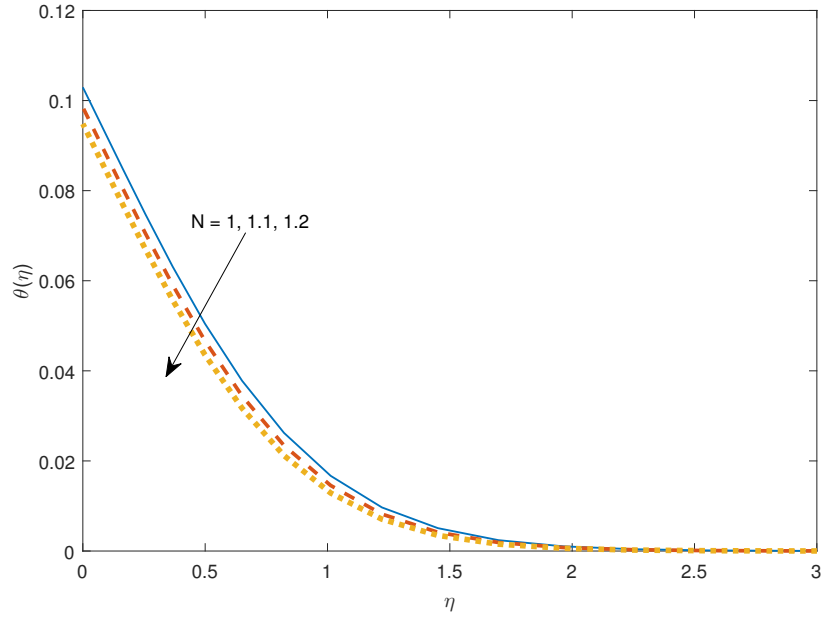

(a)

FIGURE 2.12: Effect of Conduction Radiation parameter(N) on (a) θ, when $\beta = 0.5,\ K = 1.5,\ M = 0.5,\ m = 0.1,\ Pr = 7,\ A = 0.1,\ Sc = 2$

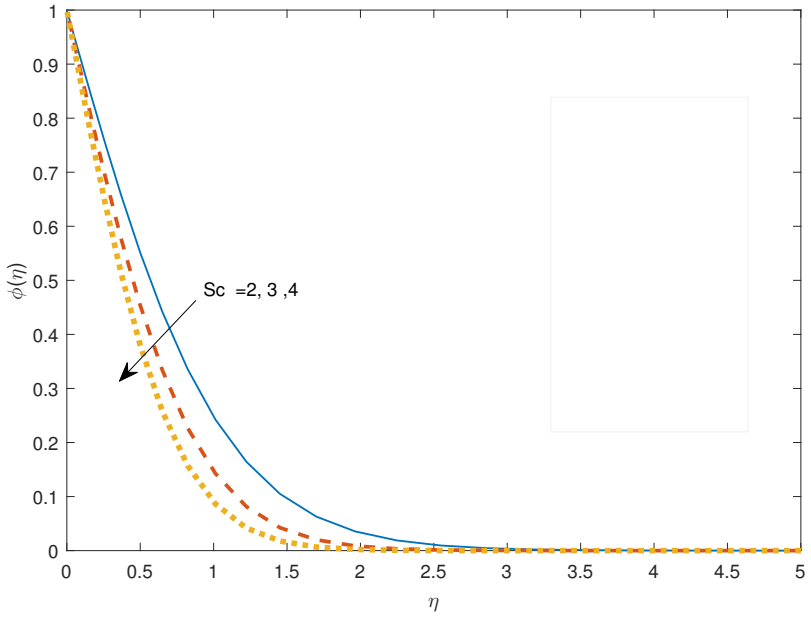

(a)

FIGURE 2.13: Effect of Sc on ϕ when $\beta = 0.5,\ K = 1.5,\ M = 0.5,\ m = 0.1,\ Pr = 7,\ N = 1,\ A = 0.1$

TABLE 2.1: Numerical Values for different physical parameters:

β	**A**	**K**	**M**	**m**	**Pr**	**N**	**Sc**	$C_f Re_x^{\frac{1}{2}}$	$-C_h Re_x^{\frac{1}{2}}$	$Nu_x Re_x^{-\frac{1}{2}}$	$-ShRe_x^{-\frac{1}{2}}$
0.5	0.1	1.5	0.5	0.1	7	1	2	0.14409694	0.02896377	1.08823232	0.96445735
1.0								0.52876634	0.03583733	1.06914865	0.94531222
1.5								0.67202067	0.03828386	1.06069716	0.93665230
0.5	0.1	1.5	0.5	0.1	7	1	2	0.14409694	0.02896377	1.08823232	0.96445735
	0.01							0.06700370	0.02838983	1.13118561	1.00016443
	0.13							0.16981684	0.02915478	1.07336376	0.95203349
0.5	0.1	1.5	0.5	0.1	7	1	2	0.14409694	0.02896377	1.08823232	0.96445735
		2						0.18369706	0.03024233	1.09319869	0.96901092
		2.5						0.21658105	0.03124973	1.09722769	0.97274242
0.5	0.1	1.5	0.5	0.1	7	1	2	0.14409694	0.02896377	1.08823232	0.96445735
			0.7					0.28358344	0.04355059	1.08081198	0.95725975
			1					0.50187350	0.06699693	1.07054791	0.94728141
0.5	0.1	1.5	0.5	0.1	7	1	2	0.14409694	0.02896377	1.08823232	0.96445735
				0.2				0.13355634	0.05595660	1.08868389	0.96489029.
				0.3				0.11736430	0.07940162	1.08939282	0.96557029
0.5	0.1	1.5	0.5	0.1	7	1	2	0.14409694	0.02896377	1.08823232	0.96445735
					10			0.14409694	-0.02896377	1.36465264	0.96445735
					15			0.14409694	0.02896377	1.74005298	0.96445735
0.5	0.1	1.5	0.5	0.1	7	1	2	0.14409694	0.02896377	1.08823232	0.96445735
						1.1		0.14409694	0.02896377	1.13269864	0.96445735
						1.2		0.14409694	0.02896377	1.17260925	0.96445735
0.5	0.1	1.5	0.5	0.1	7	1	2	0.14409694	0.02896377	1.08823232	0.96445735
							3	0.14419732	0.02896377	1.08823232	1.21553922
							4	0.14420988	0.02896377	1.08823232	1.42628311

Chapter 3

Unsteady Three-Dimensional Couple Stress Casson Nanofluid Flow with Thermal Radiation and Hall Effects

3.1 Abstract

The effects of presence of nanoparticles in the base fluid on the fluid flow problem considered in Chapter-2 is presented Chapter-3. Thus, Chapter-3 is devoted to study the transient hydromagnetic three dimensional flow of a couple stress Casson nanofluid over a linearly stretching sheet including the effects of Hall current and radiative heat transfer. The fluid flow model considered in this chapter incorporates the effect of the thermopherosis and Brownian diffusion which arise due to the presence of nanoparticles in the base fluid. The solution process is same as adopted in Chapter-2 and the results are discussed with the help of graphs and tables.

3.2 Introduction

In the previous chapter we had discussed the significance of unsteady three-dimensional magnetohydrodynamic effect on the couple stress Casson fluid with Hall current. In this chapter we will analyze the magnetohydrodynamic effect on the couple stress Casson nanofluid flow with Hall current. Nanofluid is a new kind of heat transfer medium, containing nanoparticles (1100 nm) which are uniformly and stably distributed in a base

fluid. According to Kosik the Nanofluid can be used in areas such as Heat-transfer, Tribological, Surfactant and coating, Chemical, Process/extraction, Environmental (pollution cleaning), Bio- and pharmaceutical and Medical. The flow of non-Newtonian viscoelastic nanofluid over a linearly stretching sheet under the influence of uniform magnetic field. Heat transfer characteristics are incorporated by considering the effects of nonlinear radiation and a non uniform heat source/sink was studied by Raj et al. [18]. Ganga et al. [19] had studied the Boungiorno model of nanofluid through vertical plate in the presence of internal heat absorption. He observed that in the presence of heat generation nanosolid volume fraction profile decreases with the increase in the heat absorption. Another study was made by Biswas and Ahmmed [20]. They studied the effects of Hall current and Chemical reaction on MHD unsteady heat and mass transfer of Casson nanofluid flow through the vertical plane. He observed that there is an inverse relation between Casson parameter and velocity profiles. It is also observed that with the decrease in temperature profiles, heat generation parameters decreases. Mahanthesh et. al. [21] had studied the MHD flow of nano Eyring-Powell fluid over a stretching sheet. They observed the effects of influential parameters on velocity, temperature and nanoparticles concentration fields.
The studies mentioned above do not investigate the combined effects of couple stress, thermal radiation and unsteadiness on the three dimensional flow of a Casson Nanofluid under the influence of an applied magnetic field and the resulting Hall current effects. The present chapter intends to present a numerical solution of the unsteady three dimensional MHD flow od a couple stress Casson Nanofluid in the presence of Hall current, non-linear radiative heat transfer, convective heating and mass-transfer effects.

3.3 Mathematical Formulation

We consider the three dimensional unsteady flow of viscous incompressible couple stress Casson fluid over a surface $y = 0$.In this chapter, additional nano-particles are added to the fluid. The fluid motion over the surface is caused due to a time dependent stretching of the surface in x-direction with velocity $u = U_w = \frac{ax}{1-ct}$. The fluid flow is permeated with a magnetic field $B(t)$ applied along the y-axis. The small magnetic Reynolds number assumption is taken into account to neglect the effects of induced magnetic field. However, the effects of Hall current on the flow field is retained. The surface of the sheet is heated by a hot fluid which causes a convective heat transfer with heat transfer coefficient h_s. Further, the concentration at the surface is denoted by C_f while, outside the boundary layer region, the concentration and temperature are C_∞ and T_∞ respectively.

Under the above assumptions, the equations governing the conservation of mass, momentum, energy and species concentration including the effects of Hall current, thermal radiation and couple stress, are

$$\frac{\partial u}{\partial x}+\frac{\partial v}{\partial y}+\frac{\partial w}{\partial z}=0, \tag{3.1}$$

$$\frac{\partial u}{\partial t}+u\frac{\partial u}{\partial x}+v\frac{\partial u}{\partial y}+w\frac{\partial u}{\partial z}=\left(1+\frac{1}{\beta}\right)\nu\frac{\partial^2 u}{\partial y^2}-\nu'\frac{\partial^4 u}{\partial y^4}-\frac{\sigma B^2(t)}{\rho\left(1+m^2\right)}\left(u+mw\right), \tag{3.2}$$

$$\frac{\partial w}{\partial t}+u\frac{\partial w}{\partial x}+v\frac{\partial w}{\partial y}+w\frac{\partial w}{\partial z}=\left(1+\frac{1}{\beta}\right)\nu\frac{\partial^2 w}{\partial y^2}-\nu'\frac{\partial^4 w}{\partial y^4}+\frac{\sigma B^2(t)}{\rho(1+m^2)}\left(mu-w\right), \tag{3.3}$$

$$\frac{\partial T}{\partial t}+u\frac{\partial T}{\partial x}+v\frac{\partial T}{\partial y}+w\frac{\partial T}{\partial z}=\frac{\partial}{\partial y}\left(\left(\alpha_m+\left(\frac{16\sigma^* T^3}{3\alpha^* C_p\rho}\right)\right)\frac{\partial T}{\partial y}\right)+\tau\left(D_B\frac{\partial C}{\partial y}\frac{\partial T}{\partial y}+\frac{D_T}{T_\infty}\left(\frac{\partial T}{\partial y}\right)^2\right), \tag{3.4}$$

$$\frac{\partial C}{\partial t}+u\frac{\partial C}{\partial x}+v\frac{\partial C}{\partial y}+w\frac{\partial C}{\partial z}=D\frac{\partial^2 C}{\partial y^2}+\frac{D_T}{T_\infty}\left(\frac{\partial^2 T}{\partial y^2}\right). \tag{3.5}$$

.

The suitable boundary conditions are:

$$u=u_w=\frac{ax}{1-ct}, v=0, w=0, \frac{\partial T}{\partial y}=-h_s T, C=C_f,$$

$$\frac{\partial^2 u}{\partial y^2}=0, \frac{\partial^2 w}{\partial y^2}=0.$$

at $y=0$.

$$u\to 0, w\to 0, T\to T_\infty, C\to C_\infty, \frac{\partial u}{\partial y}\to 0, \frac{\partial w}{\partial y}\to 0.$$

as $y\to\infty$.

where u, v and w are the velocities in x, y and z- directions respectively, $\nu=\frac{\mu}{\rho}$ is the kinematic viscocity, $\nu'=\frac{\eta}{\rho}$ is the couple stress viscosity, β is the Casson fluid parameter, ρ is the density, m is the Hall current, σ is the electric charge density, α_m is the thermal diffusivity, α^* is the Roseland mean absorption coefficient, σ^* is the Stefan-Boltzmann coefficient, τ is the ratio between the effective heat capacity of the nano particle material and heat capacity of the fluid, h_s is the heat transfer coefficient, D_B is the Brownian diffusion coefficient, D_T the thermophoretic diffusion coefficient, C_p is the specific heat capacity, C is the concentration of species, D is the coefficient of diffusing species, T_∞ and C_∞ are the ambient temperature and concentration respectively.

To obtain the similar form of governing equations, we use the following transformations:

$u = \frac{ax}{(1-ct)} f'(\eta)$, $v = -\sqrt{\frac{a\nu}{(1-ct)}} f(\eta)$, $w = \frac{ax}{(1-ct)} h(\eta)$,

$\eta = y\sqrt{\frac{a}{\nu(1-ct)}}$, $\theta(\eta) = \frac{T-T_\infty}{T_\infty}$, $\phi(\eta) = \frac{C-C_\infty}{C_f-C_\infty}$.

further, in order to get a similarity solution, the time dependent transverse magnetic field is chosen as:

$$B^2(t) = \frac{(B_0)^2}{1-ct}$$

.

The similarity transformations are:

$$u = \frac{ax}{(1-ct)} f'(\eta), v = -\sqrt{\frac{a\nu}{(1-ct)}} f(\eta), w = \frac{ax}{(1-ct)} h(\eta), \tag{3.6}$$

$$\eta = y\sqrt{\frac{a}{\nu(1-ct)}}, \theta(\eta) = \frac{T-T_\infty}{T_\infty}, \phi(\eta) = \frac{C-C_\infty}{C_f-C_\infty}. \tag{3.7}$$

.

The governing differential equations after using the above transformations become:

$$\left(1+\frac{1}{\beta}\right) f''' - \left(f'^2 - ff''\right) - A\left(\frac{\eta}{2} f'' + f'\right) - Kf^v - \frac{M}{1+m^2}\left(f' + hm\right) = 0, \tag{3.8}$$

$$\left(1+\frac{1}{\beta}\right) h'' - \left(f'h - fh'\right) - A\left(\frac{\eta}{2} h' + h\right) - Kh^{iv} + \frac{M}{1+m^2}\left(f'm - h\right) = 0, \tag{3.9}$$

$$\frac{1}{Pr}\theta'' - \theta'\left(A\frac{\eta}{2}\right) + \theta' f + \frac{4}{3NPr}\left(\theta'\left(\theta+1\right)^3\right)' + N_b\theta'\phi' + N_t\left(\theta'\right)^2 = 0, \tag{3.10}$$

$$\phi'' - PrLe\left(A\frac{\eta}{2} - f\right)\phi' + \frac{N_t}{N_b}\theta'' = 0. \tag{3.11}$$

The boundary conditions become:
At $y = 0$

$$f = 0, f' = 1, h = 0, \theta' = -\gamma\left(\theta+1\right), \phi = 1, f''' = 0, h'' = 0. \tag{3.12}$$

As $y \to \infty$

$$f' = 0, h = 0, f'' = 0, h' = 0, \theta = 0, \phi = 0. \tag{3.13}$$

where, $a > 0$ is the constant,

$A = \frac{c}{a}$ is the time dependent parameter,

$K = \frac{\nu' a}{\nu^2(1-ct)}$ is the couple stress parameter,

$M = \frac{\sigma(B_0)^2}{a\rho}$ is the magnetic parameter,

$Pr = \frac{\nu}{\alpha_m}$ is the Prandtl number,

$N = \frac{\rho\alpha^* C_p \alpha_m}{4\sigma^*(T_\infty)^3}$ is the conduction radiation parameter.

$N_b = \frac{\tau D_B(C_f - C_\infty)}{\nu}$ is the Brownian motion parameter.

$N_t = \frac{\tau D_T}{\nu}$ is the thermopherosis parameter.

$Le = \frac{\alpha_m}{D_B}$ is the Lewis Number.

$\gamma = h_s\sqrt{\frac{\nu(1-ct)}{a}}$ is the conjugate parameter for Newtonian heating.

Skin friction along the x and z directions, Nusselt number and Sherwood number are given by:

$C_f Re_x^{\frac{1}{2}} = \left(1 + \frac{1}{\beta}\right) f"(0) - Kf^v(0)$, $C_h Re_x^{\frac{1}{2}} = \left(1 + \frac{1}{\beta}\right) h'(0) - Kh^{iv}(0)$,

$Nu_x Re_x^{-\frac{1}{2}} = \gamma\left(1 + \frac{4(1+\theta(0))^3}{3N}\right)\left(1 + \frac{1}{\theta(0)}\right)$, $ShRe_x^{-\frac{1}{2}} = -\phi'(0)$.

3.4 Numerical Solution

The numerical solution of couple non-linear ordinary differential equations (3.8)-(3.11) subject to boundary conditions (3.12)-(3.13) is obtained by "Spectral Quasi Linearlisation Method". For this we assume,

$$L_1 = \left(1 + \frac{1}{\beta}\right) f''' - \left(f'^2 - ff''\right) - A\left(\frac{\eta}{2}f'' + f'\right) - Kf^v - \frac{M}{1+m^2}\left(f' + hm\right),$$

$$L_2 = \left(1 + \frac{1}{\beta}\right) h'' - \left(f'h - fh'\right) - A\left(\frac{\eta}{2}h' + h\right) - Kh^{iv} + \frac{M}{1+m^2}\left(f'm - h\right),$$

$$L_3 = \frac{1}{Pr}\theta'' - \theta'\left(A\frac{\eta}{2}\right) + \theta' f + \frac{4}{3NPr}\left(\theta'\left(\theta+1\right)^3\right)',$$

$$L_4 = \frac{1}{Sc}\phi'' - \phi'\left(A\frac{\eta}{2} - f\right).$$

The linear equation can be represented as

$$a_{11}^{(5)} f^v + a_{11}^{(4)} f^{iv} + a_{11}^{(3)} f''' + a_{11}^{(2)} f'' + a_{11}^{(1)} f' + a_{11}^{(0)} f + a_{12}^{(0)} h = R_1$$

where,

$$a_{11}^{(5)} = \frac{\partial L_1}{\partial f^v} = -K,$$

$$a_{11}^{(4)} = \frac{\partial L_1}{\partial f^{iv}} = 0,$$

$$a_{11}^{(3)} = \frac{\partial L_1}{\partial f^3} = \left(1 + \frac{1}{\beta}\right),$$

$$a_{11}^{(2)} = \frac{\partial L_1}{\partial f^2} = f - \frac{A\eta}{2},$$

$$a_{11}^{(1)} = \frac{\partial L_1}{\partial f^1} = -2f'f'' - A - \frac{M}{1+m^2},$$

$$a_{11}^{(0)} = \frac{\partial L_1}{\partial f} = f''$$

$$a_{12}^{(0)} = \frac{\partial L_1}{\partial h} = -\frac{Mm}{1+m^2},$$

$$R_1 = \sum_{i=0}^{5} \frac{\partial L_1}{\partial f^i} f^i + \sum_{i=0}^{5} \frac{\partial L_1}{\partial h^i} h^i - L_1 = ff'' + \left(f'\right)^2 - 2\left(f'\right)^2 f''.$$

The second linear equation for L_2 is as follows:

$$a_{22}^{(4)} h^{iv} + a_{22}^{(3)} h''' + a_{22}^{(1)} h' + a_{22}^{(0)} h + a_{21}^{(1)} f' + a_{21}^{(0)} f = R_2$$

where,

$$a_{22}^{(4)} = \frac{\partial L_2}{\partial h^{iv}} = -K,$$

$$a_{22}^{(3)} = \frac{\partial L_2}{\partial h'''} = 0,$$

$$a_{22}^{(2)} = \frac{\partial L_2}{\partial h''} = \left(1 + \frac{1}{\beta}\right),$$

$$a_{22}^{(1)} = \frac{\partial L_2}{\partial h'} = f - \frac{A\eta}{2},$$

$$a_{22}^{(0)} = \frac{\partial L_2}{\partial h} = -f' - A - \frac{M}{1+m^2},$$

$$a_{21}^{(1)} = \frac{\partial L_2}{\partial f'} = -h + \frac{Mm}{1+m^2},$$

$$a_{21}^{(0)} = \frac{\partial L_2}{\partial f} = h',$$

$$R_2 = \sum_{i=0}^{5} \frac{\partial L_2}{\partial f^i} f^i + \sum_{i=0}^{5} \frac{\partial L_2}{\partial h^i} h^i - L_2 = -hf' + h'f.$$

Now, the third linear equation is represented as:

$$a_{33}^{(2)}\theta'' + a_{33}^{(1)}\theta' + a_{33}^{(0)}\theta + a_{31}^{(0)} f + a_{34}^{(1)}\phi' = R_3$$

where,

$$a_{33}^{(2)} = \frac{\partial L_3}{\partial \theta''} = \frac{1}{Pr} + \frac{4(\theta+1)^3}{3NPr},$$

$$a_{33}^{(1)} = \frac{\partial L_3}{\partial \theta'} = -\frac{A\eta}{2} + f + \frac{8(\theta+1)^2\theta'}{NPr} + N_b\phi' + 2N_t\theta',$$

$$a_{33}^{(0)} = \frac{\partial L_3}{\partial \theta} = \frac{4(\theta+1)\left((\theta+1)\theta'' + 2\theta'^2\right)}{NPr},$$

$$a_{34}^{(1)} = \frac{\partial L_3}{\partial \phi'} = N_b\theta',$$

$$R_3 = \frac{N_bNPr\theta'\phi' + NPrf\theta' + (\theta')^2\left(NPrN_t + 12(\theta)^2 + 16\theta + 4\right) + 4\theta\left((\theta+1)^2\theta''\right)}{NPr}.$$

Now the fourth linear equation can be represented as:

$$a_{44}^{(2)}\phi'' + a_{44}^{(1)}\phi' + a_{44}^{(0)}\phi + a_{41}^{(0)} f + a_{43}^{(2)}\theta'' = R_4$$

where,

$$a_{44}^{(2)} = \frac{\partial L_4}{\partial \phi''} = 1,$$

$$a_{44}^{(1)} = \frac{\partial L_4}{\partial \phi'} = -LePr\left(\frac{A\eta}{2} - f\right),$$

$$a_{44}^{(0)} = \frac{\partial L_4}{\partial \phi} = 0,$$

$$a_{43}^{(2)} = \frac{\partial L_4}{\partial \theta''} = \frac{N_t}{N_b},$$

$$R_4 = LePrf\phi'.$$

3.5 Results and Conclusions

In this section the graphical and tabulated form of results are being discussed. These graphs are plotted using MATLAB techniques. The same values of the parameters are pre-set for the velocity, temperature and concentration profiles for the first case. Other values are changed accordingly. The same values are as follows: Casson fluid parameter (β) = 0.1, Time dependent parameter (A) = 0.01, Couple stress parameter (K) = 0.5, Magnetic field parameter (M) = 5, Hall current effect (m) = 0.1, Prandtl number (Pr) = 3, Conduction radiation parameter (N) = 1, Thermopherosis parameter (N_t) = 0.1, Brownian motion parameter ($N_b = 0.1$), Lewis number (Le) = 5.

The fig(3.1) shows the relation between Couple stress parameter and velocity components in x- and z-directions. These graphs depicts that there is positive relation between the couple stress parameter and velocity profiles.

Fig(3.2) portraits the effects of couple stress parameter on temperature and concentration profiles. It is analyzed that increase in couple stress parameter causes a decrease in temperature and concentration profiles.

The effect of Casson fluid parameter can be seen in the fig(3.3-3.4). It is clearly seen from the fig(3.3(a) & (b)) that as the Casson parameter rises, the velocity profiles shows decreasing behaviour. Whereas fig(3.4(a) & (b)) portraits that as Casson fluid parameter rises, the temperature of the fluid and concentration profiles also rises.

Fig(3.5) are prepared for the effects of time dependent parameter on the velocity components. It is evident from the figures that an increase in time dependent parameter declines the velocity components along the x- and z- directions. This happens due to the fact that the time dependent parameter is inversely proportion to the stretching coefficient. Thus an enhancement in time dependent parameter reduces the stretching ratio and a consequence the velocity minimizes.

The influence of time dependent parameter on temperature and concentration profiles is depicted in the fig(3.6).It is observed that as the time dependent parameter increases, both the profiles also increases significantly.

The dimensionless velocity distributions $f'(\eta)$ and $h(\eta)$ for different values of magnetic number are sketched in fig(3.7-3.8). It is observed that an increase in Magnetic number results in reducing the velocity profile in both x- and z- directions. This retardation in momentum boundary layer thickness is due to the presence of Lorentz force. It is also known that, the Lorentz force is stronger corresponding to larger magnetic parameter which oppose the motion of the fluid and hence some useful energy is converted into heat due to frictional forces.

The effects of Magnetic parameter on temperature and concentration profiles can be seen in fig(3.8(a) & (b)). Unlike velocity distributions, temperature and concentration shows a same behaviour as a change in Magnetic number, i.e.,with the rise in magnetic

number, both the profiles also rises.

The effect of the hall current on velocity, concentration and temperature profiles can be seen in the figures(3.9-3.10). It is seen from the graphs that there is a positive relation between the Hall current effect and velocity profiles. With the increase in Hall effect the velocity graph in x- and z-directions shows a rising trend as that of Hall effect. On the contrary temperature and concentration graphs shows a declining trend with the increase in Hall effect.

Effect of Prandtl number on temperature and concentration profile can be seen in the fig(3.11). Since Prandtl number is the ratio of the viscous diffusion rate to the thermal diffusion rate, higher the values of Prandtl number reduce the thermal diffusivity. Consequently, for increasing values of Prandtl number decreases the temperature profile is depicted in the fig(3.11(a)). Similarly, the concentration profile shows a declining trend when there is a increase in Prandtl number.

The temperature fluid decreases when there is a increase in conduction radiation parameter. It is clearly seen in the fig(3.12).

When the thermopherosis parameter increases, the temperature and concentration profiles shows a rising trend. This is shown in the fig(3.13).

There is a enhancement in temperature profile while there is a declining trend in the concentration profile with the increase in Brownian motion parameter. This can be observed from the fig(3.14).

The effect of Lewis number is opposite on both the temperature and concentration profiles. The concentration profile graph shows a decreasing behaviour when the Lewis number is increasing. While the temperature increases with the increase in Lewis number.

The effect of the pertinent flow parameters such as the Casson parameter (β), unsteadiness parameter (A), couple stress parameter (K), magnetic parameter (M), Hall current parameter (m), Prandtl number (Pr), radiation parameter (N), Brownian motion parameter (N_b), Thermopherosis parameter (N_t) and Lewis number (Le) on the skin-friction coefficients in x- and z- directions presented in Table 3.1 whereas the effect on Nusselt number and Sherwood number are presented in Table 3.2. It is analyzed from first table that skin-friction coefficient in x-direction increases with the increase in following parameters: β, A, K, M. On the other hand, skin-friction coefficient in z-direction decreases with increase in β, A, K, M, Pr, N_t. The effect of Hall current in x- and z-directions on skin-friction decreases with the increase in Hall current followed by increase in skin-friction in z-direction. The skin-friction coefficient in x- and z-direction shows opposite results in case of radiation parameter. It decreases in x-direction but increases in z-direction with the increase in N. The skin-friction coefficient in z-direction increases in case of N_b and Le. With the increase in Pr, N_t, N_b and Le, the skin-friction coefficient first decreases then increases.

The Nusselt number is increased for β, Hall current (m) and Pr with their increase, whereas the Sherwood number decreases for these parameters. The Sherwood number and Nusselt number both increases with the increase in radiation parameter. With the increase in N_b and Le both Sherwood number and Nusselt number decreases. The Nusselt number decreases whereas Sherwood number increases with the increase in A, K, M and N_t.

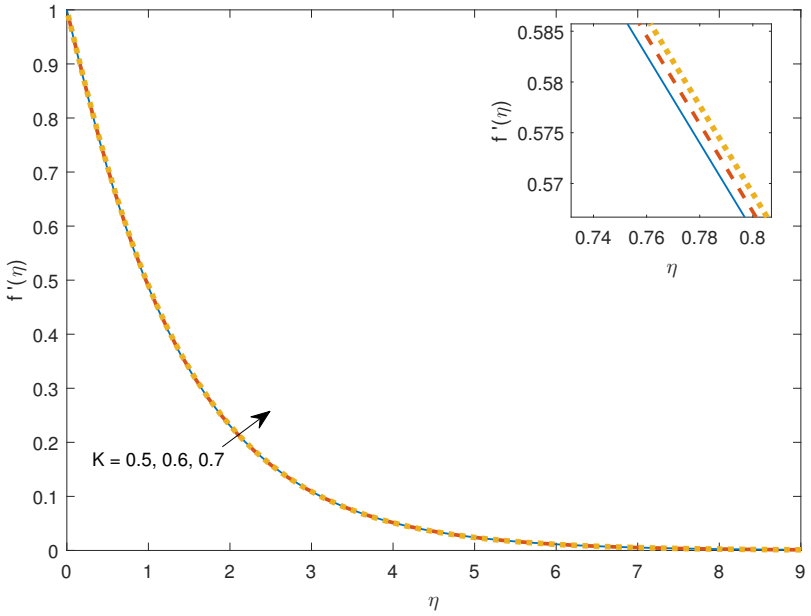

(a)

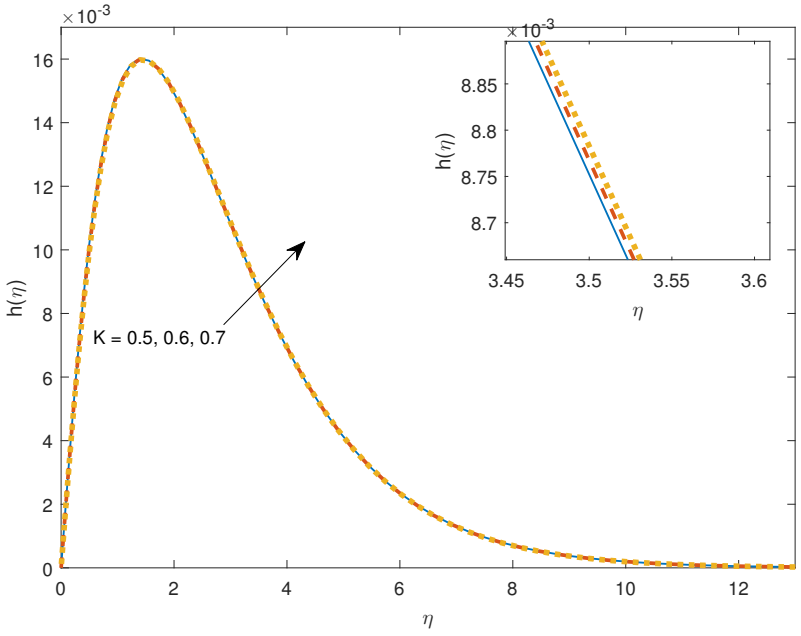

(b)

FIGURE 3.1: Effect of Couple stress parameter(K) on (a) f', (b) h when $\beta = 0.1,\ A = 0.01,\ M = 5,\ m = 0.1,\ Pr = 3,\ N = 1,\ N_t = 0.1,\ N_b = 0.1,\ Le = 5$

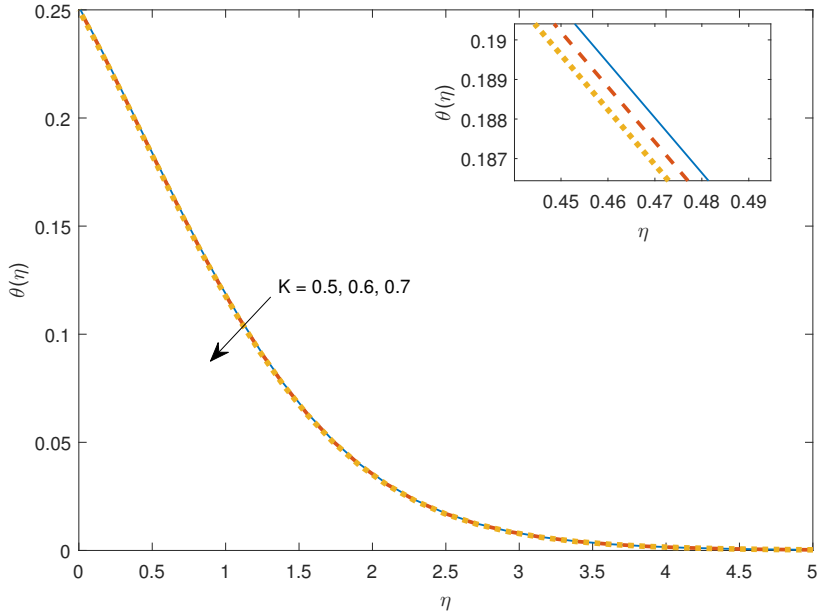

(a)

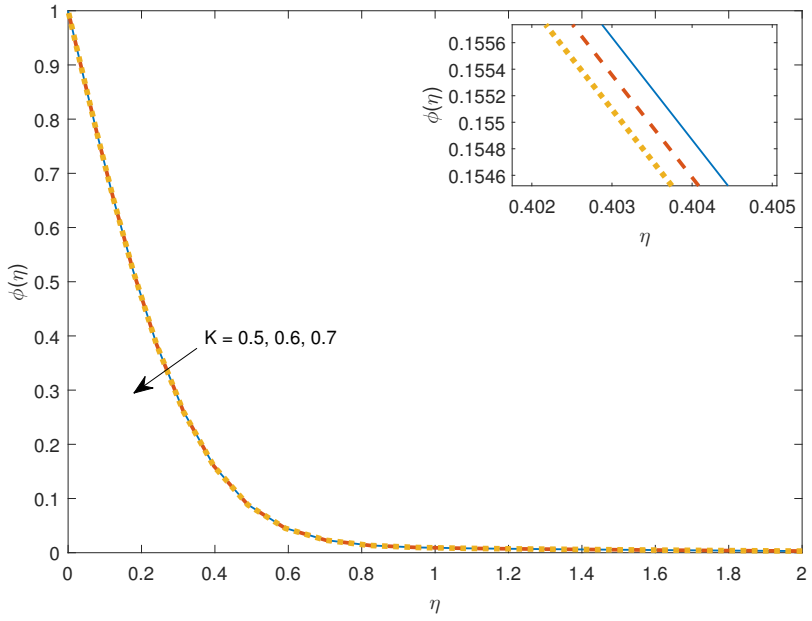

(b)

FIGURE 3.2: Effect of Couple stress parameter(K) on (a) θ, (b) ϕ when $\beta = 0.1,\ A = 0.01,\ M = 5,\ m = 0.1,\ Pr = 3,\ N = 1,\ N_t = 0.1,\ N_b = 0.1,\ Le = 5$

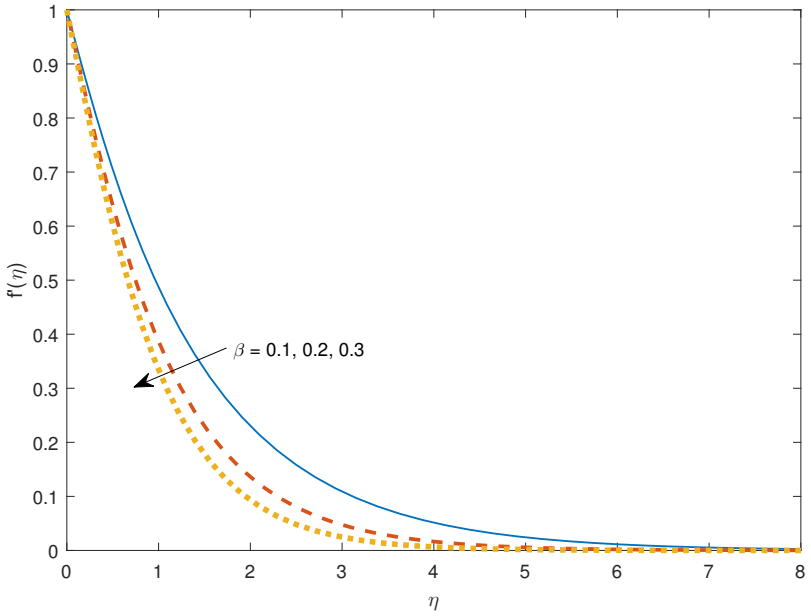

(a)

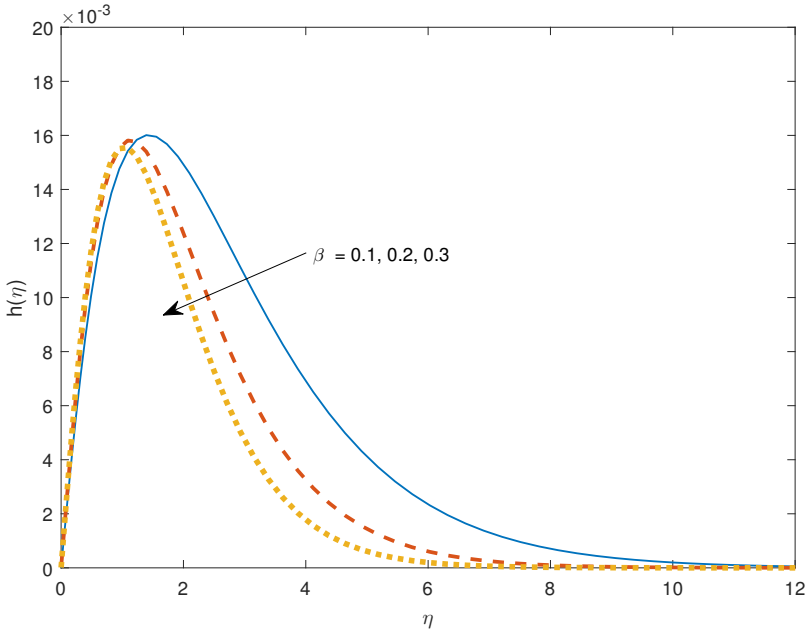

(b)

FIGURE 3.3: Effect of Casson Fluid Parameter (β) on (a) f', (b) h when $K = 0.5,\ A = 0.01,\ M = 5,\ m = 0.1,\ Pr = 3,\ N = 1,\ N_t = 0.1,\ N_b = 0.1,\ Le = 5$

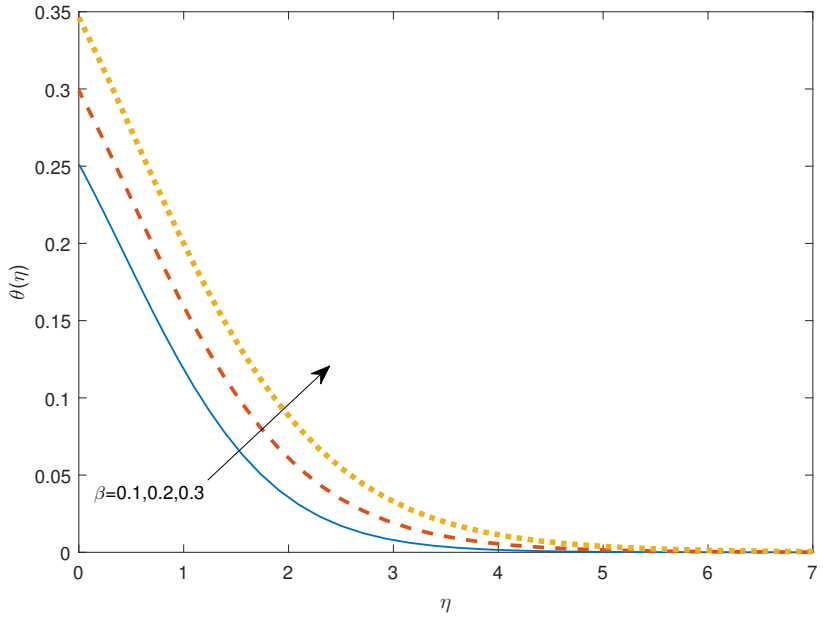

(a)

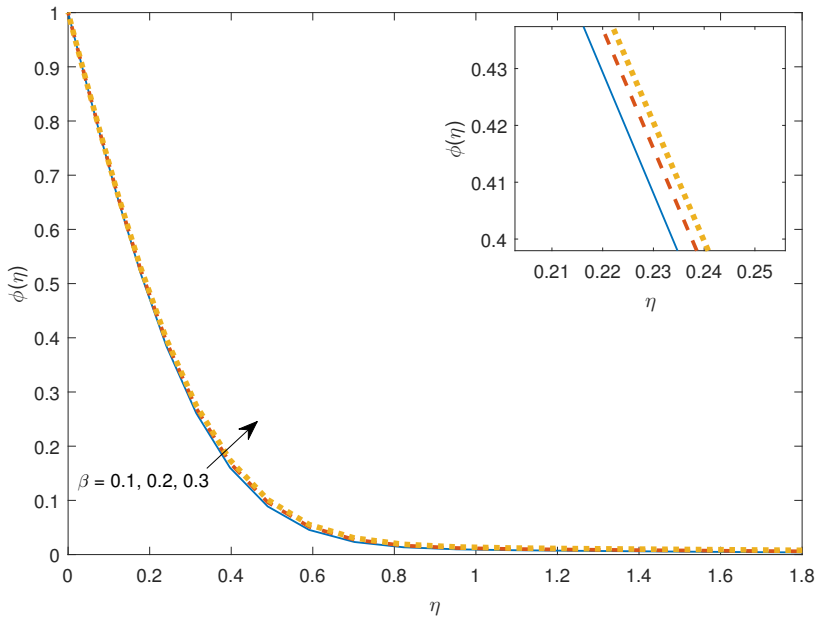

(b)

FIGURE 3.4: Effect of Casson Fluid Parameter (β) on (a) θ, (b) ϕ when $K = 0.5,\ A = 0.01,\ M = 5,\ m = 0.1,\ Pr = 3,\ N = 1,\ N_t = 0.1,\ N_b = 0.1,\ Le = 5$

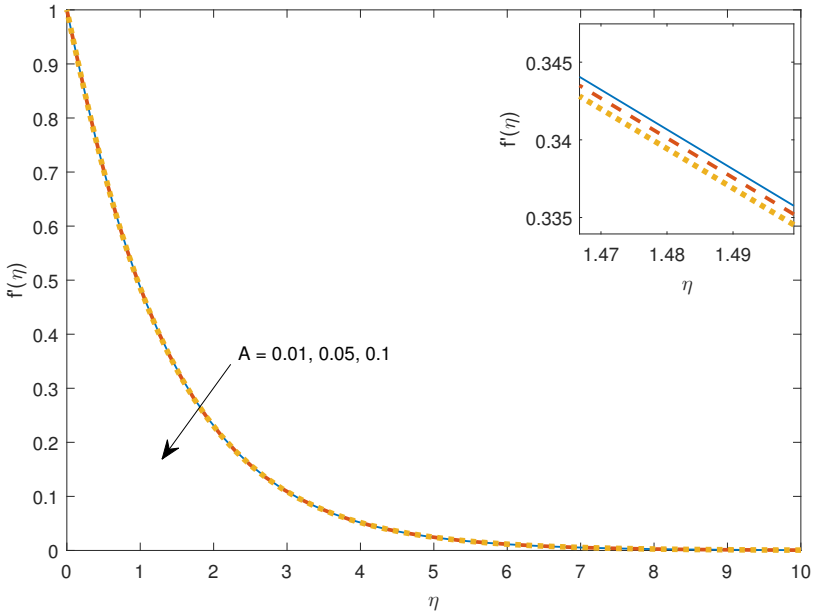

(a)

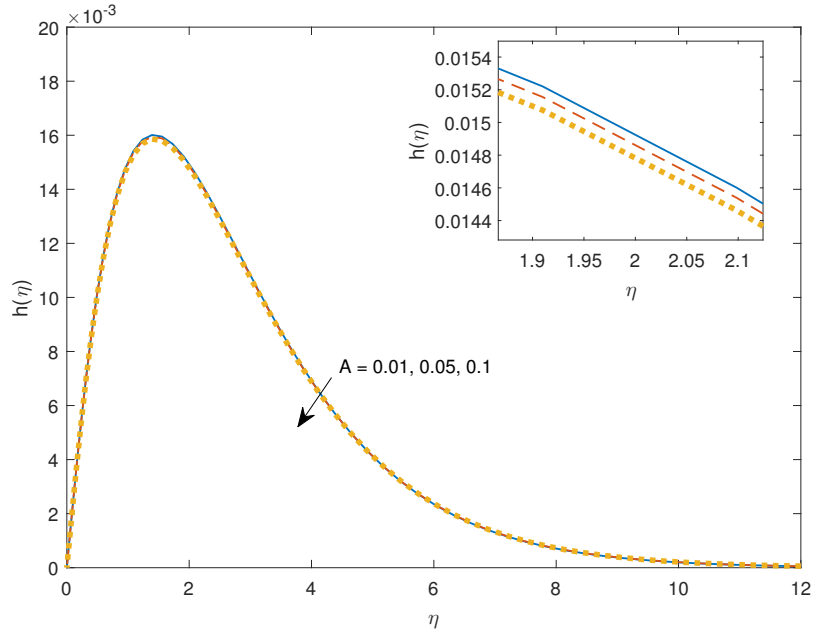

(b)

FIGURE 3.5: Effect of A on (a) f', (b) h when $\beta = 0.1,\ K = 0.5,\ M = 5,\ m = 0.1,\ Pr = 3,\ N = 1,\ N_t = 0.1,\ N_b = 0.1,\ Le = 5$

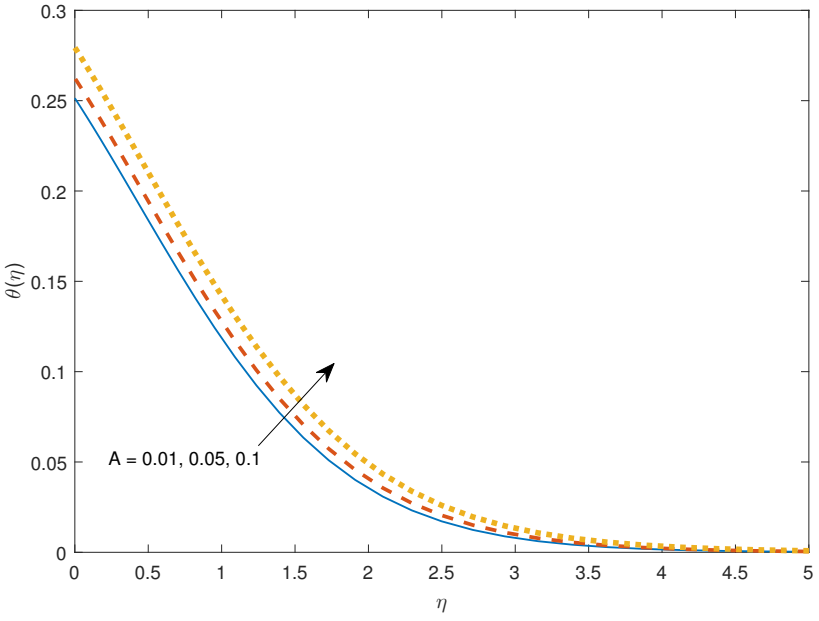

(a)

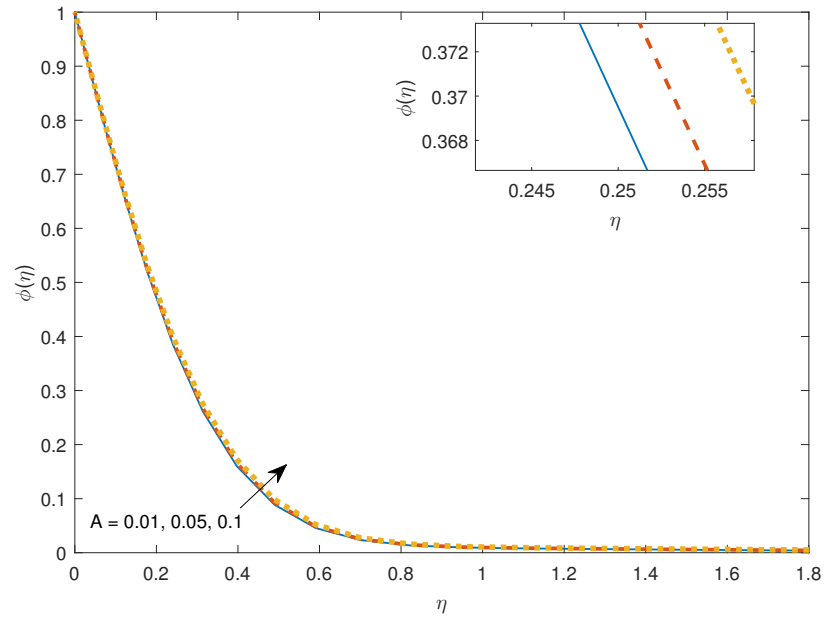

(b)

FIGURE 3.6: Effect of A on (a) θ, (b) ϕ when $\beta = 0.1$, $K = 0.5$, $M = 5$, $m = 0.1$, $Pr = 3$, $N = 1$, $N_t = 0.1$, $N_b = 0.1$, $Le = 5$

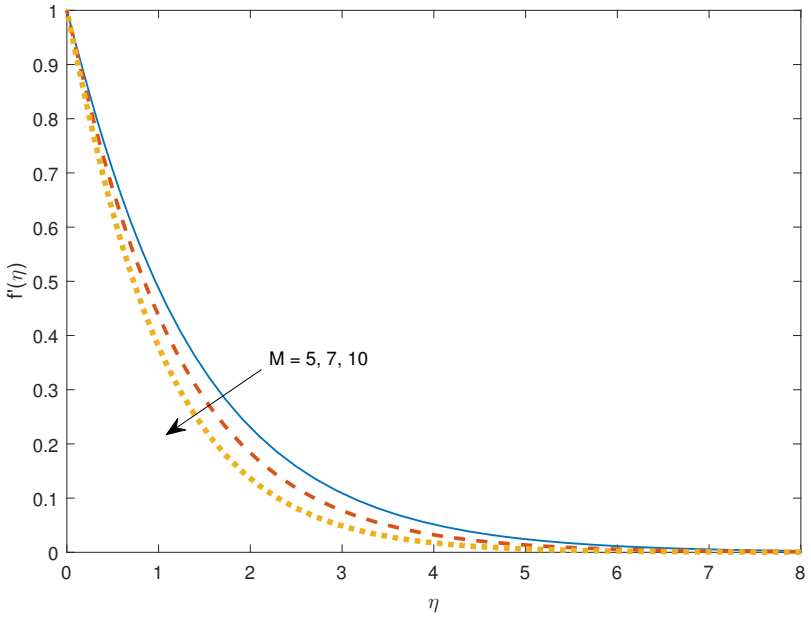

(a)

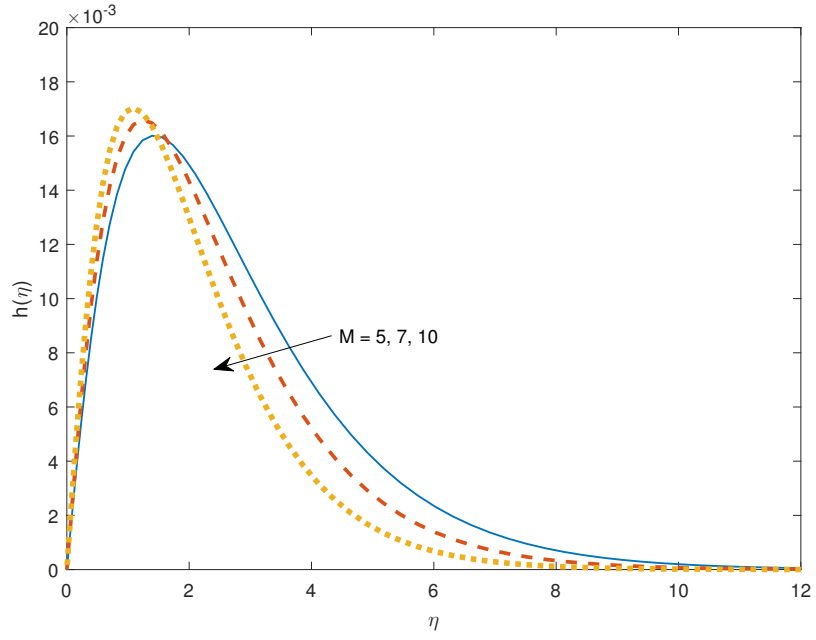

(b)

FIGURE 3.7: Effect of Magnetic Radiation (M) on (a) f', (b) h when $\beta = 0.1,\ A = 0.01,\ K = 0.5,\ m = 0.1,\ Pr = 3,\ N = 1,\ N_t = 0.1,\ N_b = 0.1,\ Le = 5$

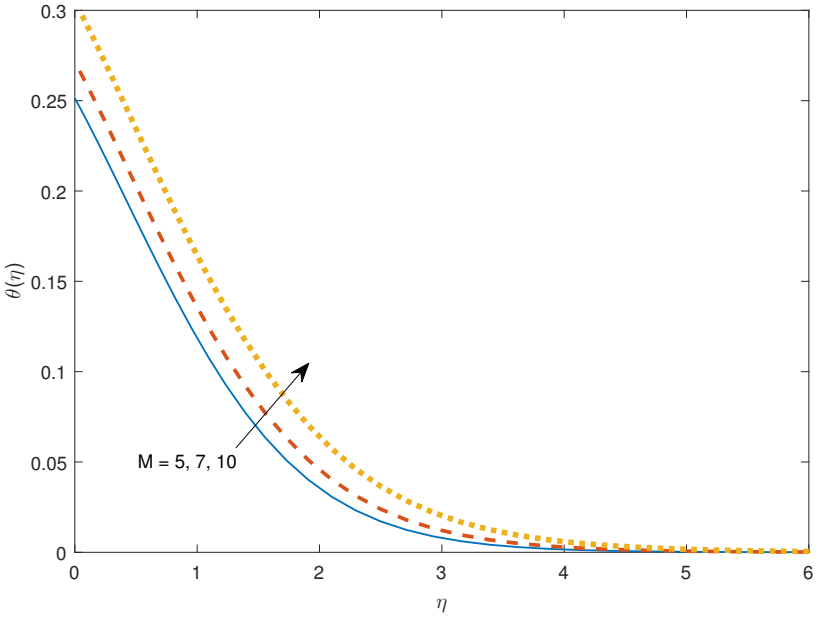

(a)

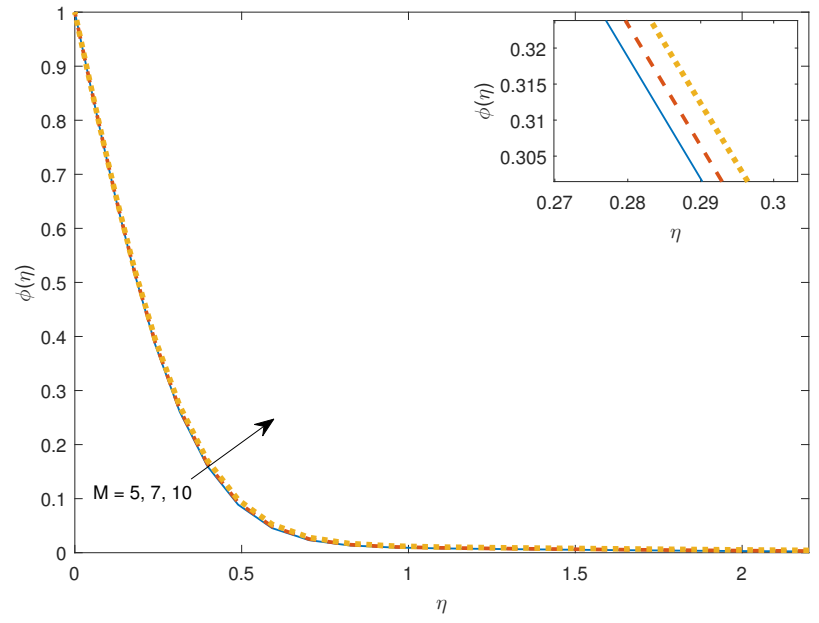

(b)

FIGURE 3.8: Effect of Magnetic Radiation (M) on (a) θ, (b) ϕ when $\beta = 0.1,\ A = 0.01,\ K = 0.5,\ m = 0.1,\ Pr = 3,\ N = 1,\ N_t = 0.1,\ N_b = 0.1,\ Le = 5$

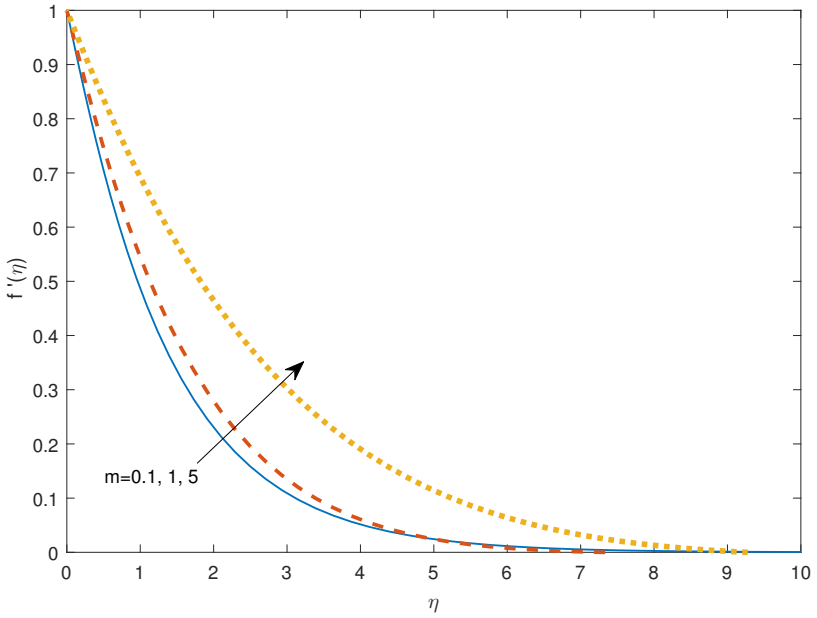

(a)

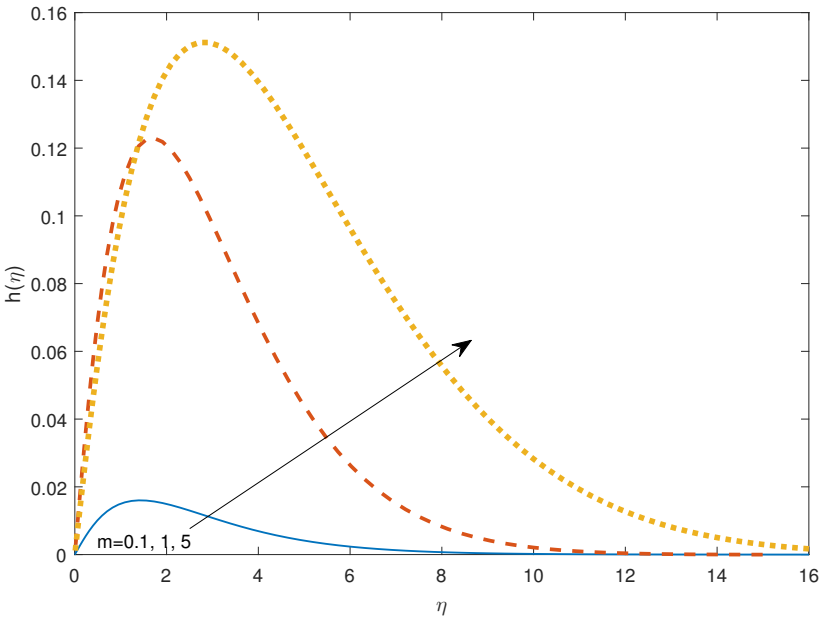

(b)

FIGURE 3.9: Effect of Hall Current Effect (m) on (a) f', (b) h when $\beta = 0.1,\ A = 0.01,\ M = 5,\ K = 0.5,\ Pr = 3,\ N = 1,\ N_t = 0.1,\ N_b = 0.1,\ Le = 5$

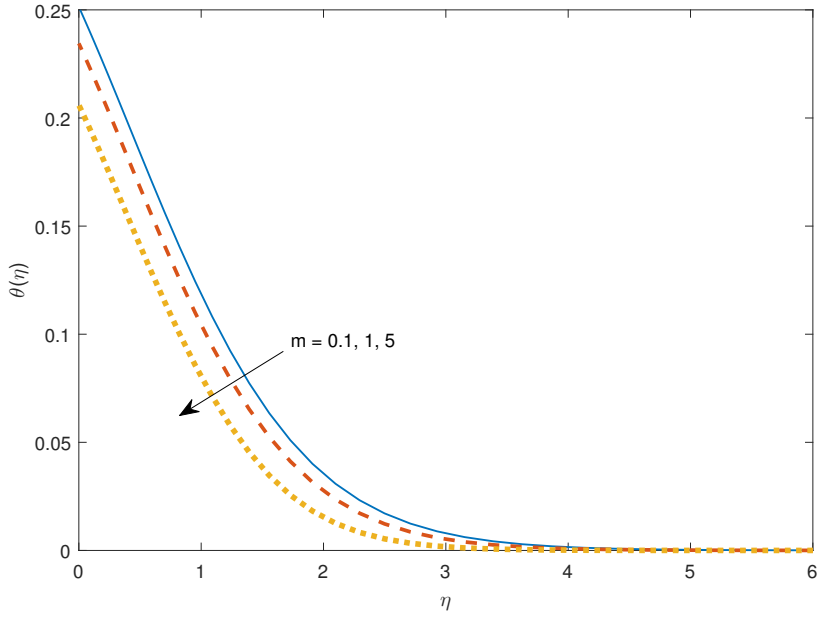

(a)

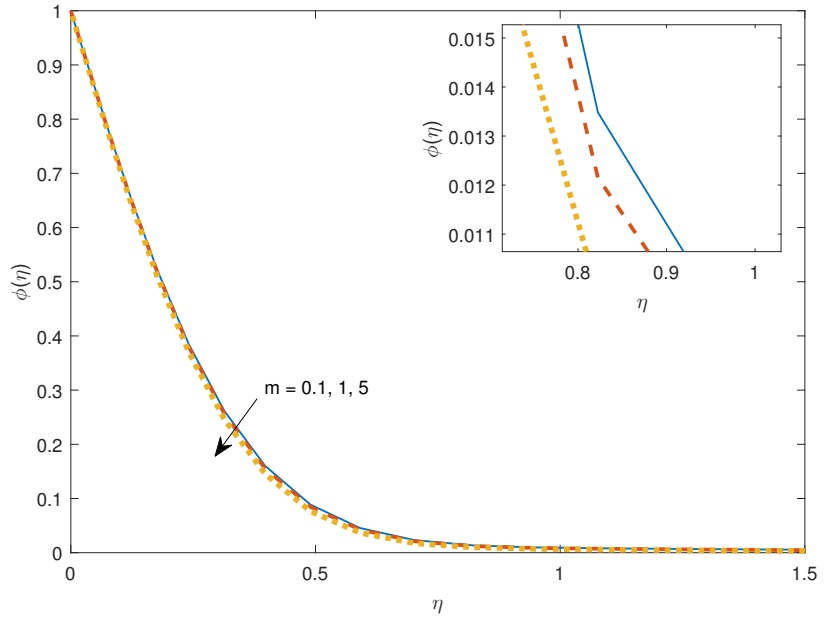

(b)

FIGURE 3.10: Effect of Hall Current Effect (m) on (a) θ, (b) ϕ when $\beta = 0.1,\ A = 0.01,\ M = 5,\ K = 0.5,\ Pr = 3,\ N = 1,\ N_t = 0.1,\ N_b = 0.1,\ Le = 5$

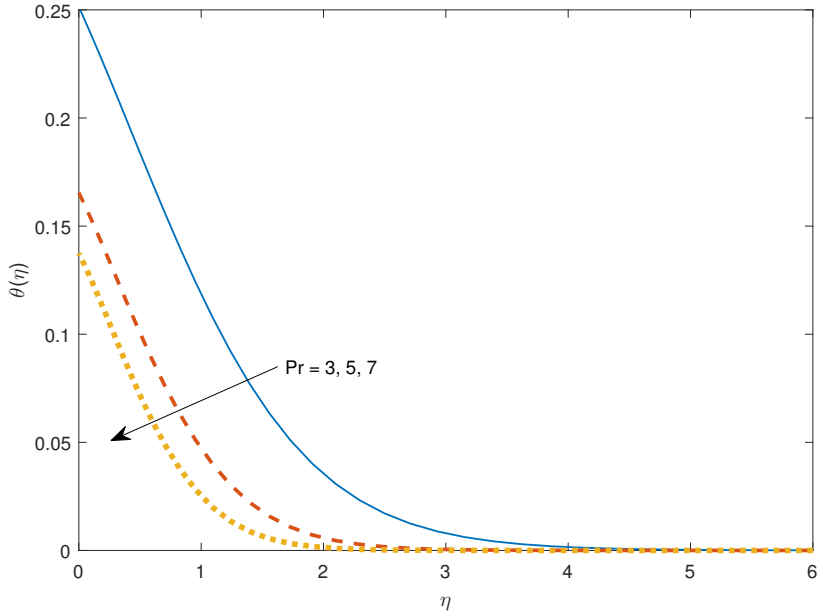

(a)

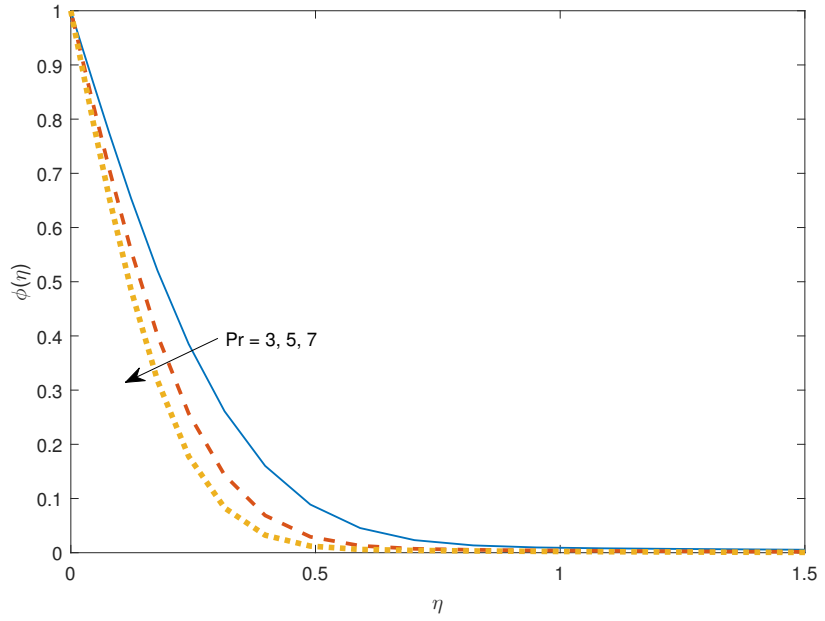

(b)

FIGURE 3.11: Effect of Pr on (a) θ, (b) ϕ when $\beta = 0.1,\ A = 0.01,\ M = 5,\ m = 0.1,\ K = 0.5,\ N = 1,\ N_t = 0.1,\ N_b = 0.1,\ Le = 5$

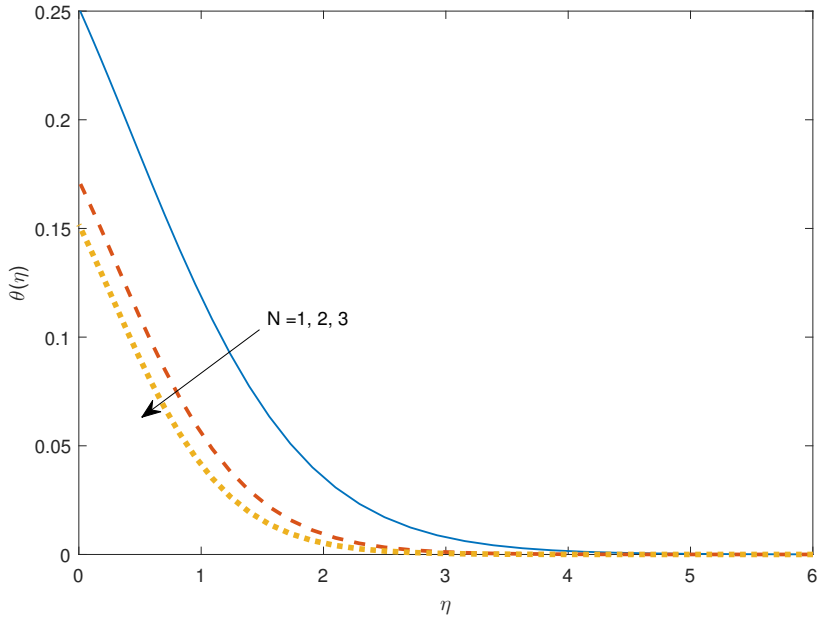

(a)

FIGURE 3.12: Effect of N on θ, when $\beta = 0.1,\ A = 0.01,\ M = 5,\ m = 0.1,\ Pr = 3,\ K = 0.5,\ N_t = 0.1,\ N_b = 0.1,\ Le = 5$

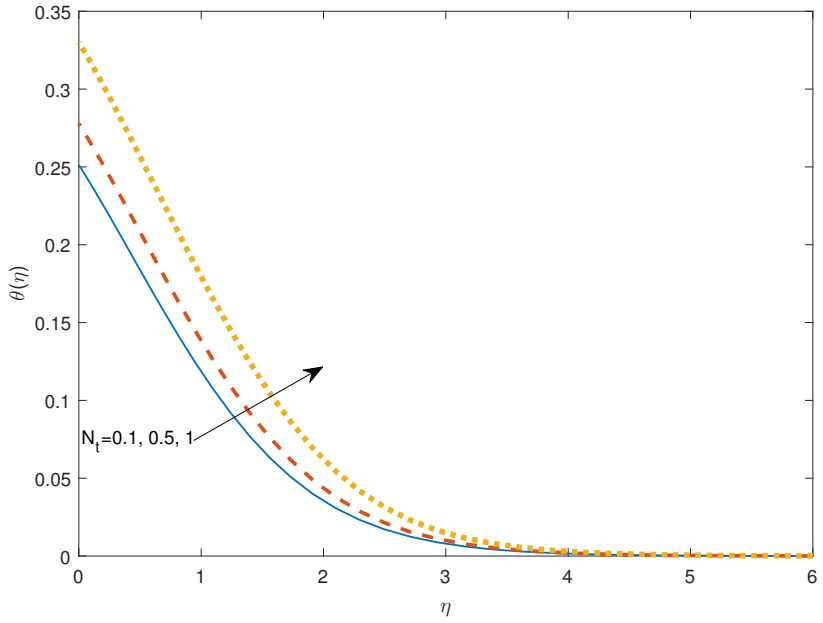

(a)

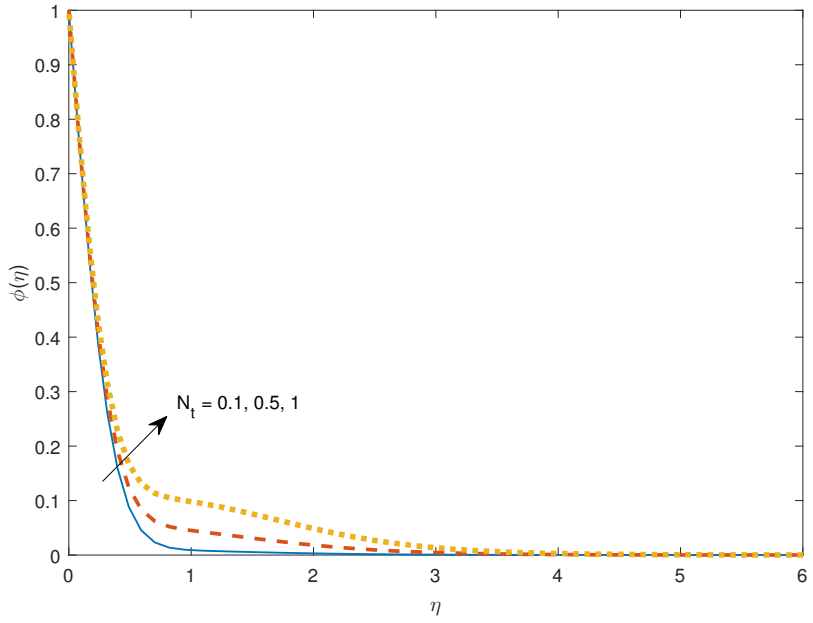

(b)

FIGURE 3.13: Effect of N_t on (a) θ, (b) ϕ when $\beta = 0.1,\ A = 0.01,\ M = 5,\ m = 0.1,\ Pr = 3,\ N = 1,\ K = 0.5,\ N_b = 0.1,\ Le = 5$

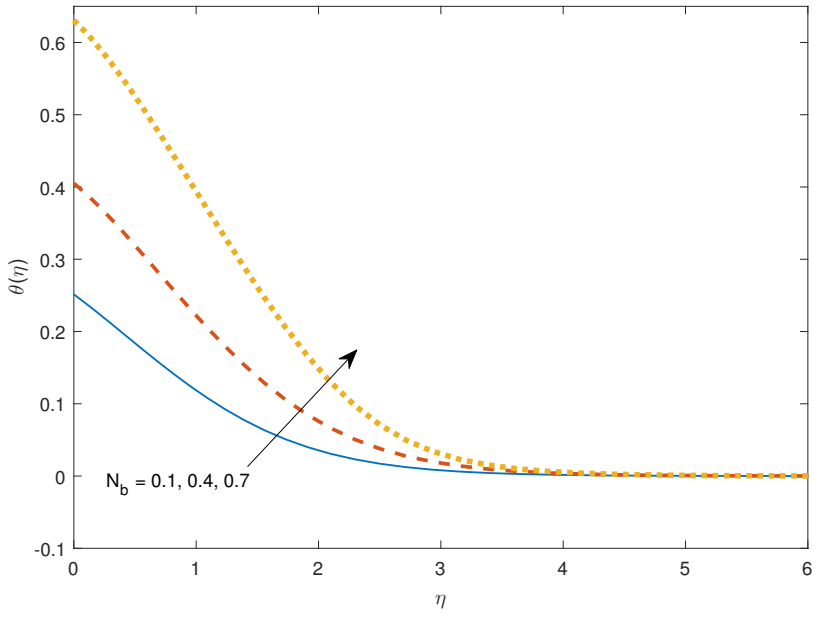

(a)

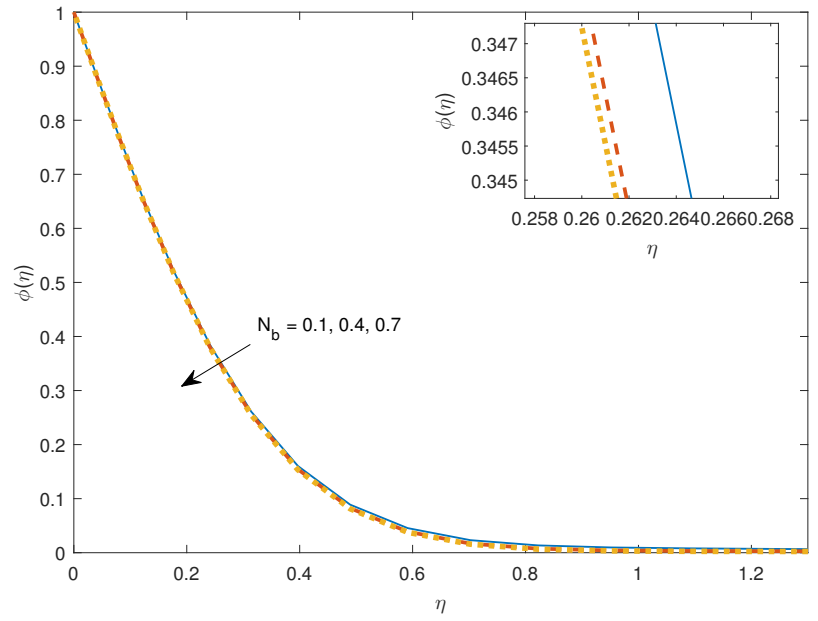

(b)

FIGURE 3.14: Effect of N_b on (a) θ, (b) ϕ when $\beta = 0.1,\ A = 0.01,\ M = 5,\ m = 0.1,\ Pr = 3,\ N = 1,\ N_t = 0.1,\ K = 0.5,\ Le = 5$

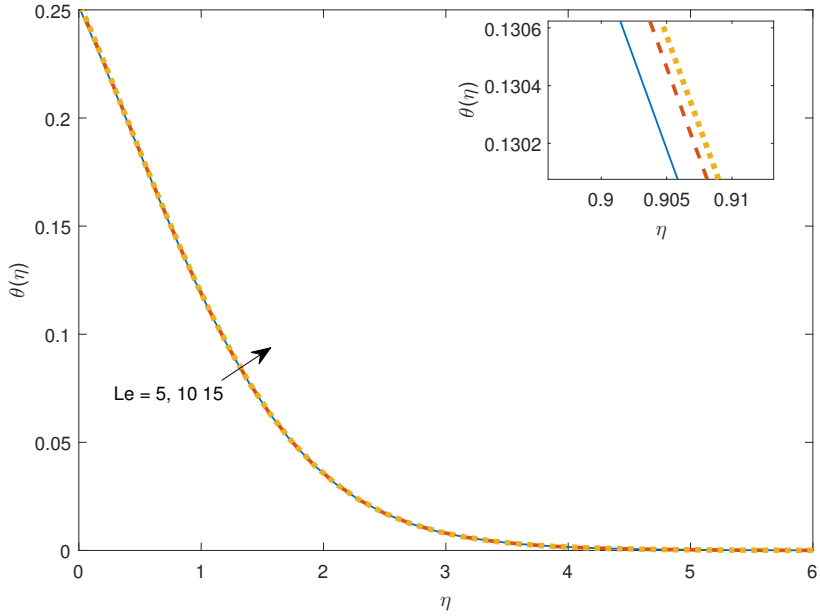

(a)

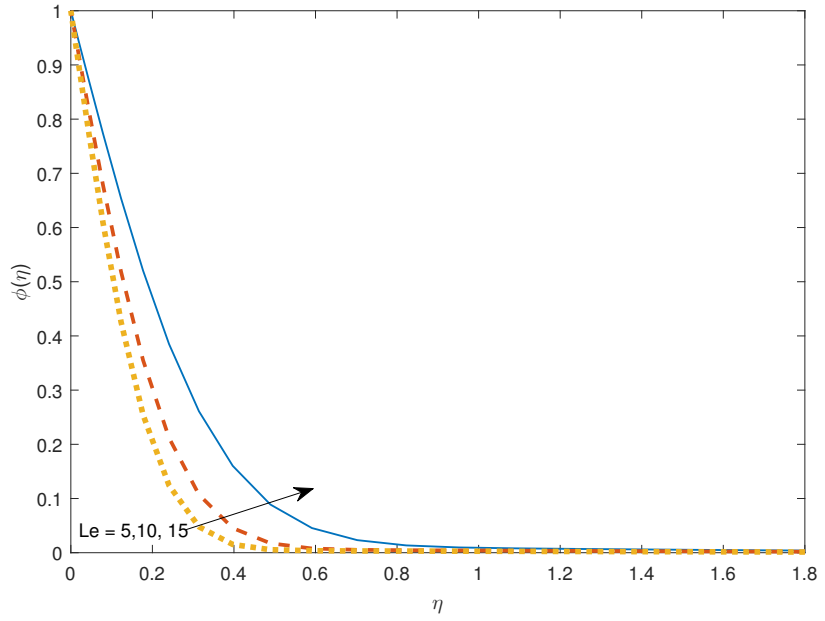

(b)

FIGURE 3.15: Effect of Le on (a) θ, (b) ϕ when $\beta = 0.1,\ A = 0.01,\ M = 5,\ m = 0.1,\ Pr = 3,\ N = 1,\ N_t = 0.1,\ N_b = 0.1,\ K = 0.5$

TABLE 3.1: Numerical Values for different physical parameters:

β	**A**	**K**	**M**	**m**	**Pr**	**N**	N_t	N_b	**Le**	$-C_f Re_x^{\frac{1}{2}}$	$-C_h Re_x^{\frac{1}{2}}$
0.1	0.01	0.5	5	0.1	3	1	0.1	0.1	5	0.52178173	0.23866437
0.2										0.49733602	0.24309379
0.3										0.46908376	0.24709283
0.5	0.01	0.5	5	0.1	3	1	0.1	0.1	5	0.52178173	0.23866437
	0.05									0.49313188	0.23946942
	0.1									0.45712009	0.24046953
0.5	0.01	0.5	5	0.1	3	1	0.1	0.1	5	0.52178173	0.23866437
		0.6								-1.59070801	0.33460475
		0.7								-2.48477464	0.37361674
0.5	0.01	0.5	5	0.1	3	1	0.1	0.1	5	0.52178173	0.23866437
			7							-0.69326339	0.39708897
			10							-2.75215689	0.64951381
0.5	0.01	0.5	5	0.1	3	1	0.1	0.1	5	0.52178173	0.23866437
				1						2.07085866	0.79978713
				5						2.40788345	-0.36244148
0.5	0.01	0.5	5	0.1	3	1	0.1	0.1	5	0.52178173	0.23866437
					5					0.52251859	0.23866436
					7					0.52208105	0.23866440
0.5	0.01	0.5	5	0.1	3	1	0.1	0.1	5	0.52178173	0.23866437
						2				0.52299687	0.23866437
						3				0.52302114	0.23866440
0.5	0.01	0.5	5	0.1	3	1	0.1	0.1	5	0.52178173	0.23866437
							0.5			0.52299251	0.23866439
							1			0.52198662	0.23866439
0.5	0.01	0.5	5	0.1	3	1	0.1	0.1	5	-0.50452099	2.91836987
								0.4		0.52337024	0.23866440
								0.7		0.52242344	0.23866436
0.5	0.01	0.5	5	0.1	3	1	0.1	0.1	5	-0.50452099	2.91836987
									10	0.52187894	0.23866437
									15	0.52154665	0.23866439

TABLE 3.2: Numerical Values for different physical parameters:

β	**A**	**K**	**M**	**m**	**Pr**	**N**	N_t	N_b	**Le**	$Nu_x Re_x^{-\frac{1}{2}}$	$-ShRe_x^{-\frac{1}{2}}$
0.1	0.01	0.5	5	0.1	3	1	0.1	0.1	5	0.50452099	2.91836987
0.2										0.50555520	2.91986648
0.3										0.50653310	2.92122340
0.5	0.01	0.5	5	0.1	3	1	0.1	0.1	5	0.50452099	2.91836987
	0.05									0.48744291	2.88316334
	0.1									0.46412636	2.83831497
0.5	0.01	0.5	5	0.1	3	1	0.1	0.1	5	0.50452099	2.91836987
		0.6								0.44047149	2.87672383.
		0.7								0.39424932	2.85261119.
0.5	0.01	0.5	5	0.1	3	1	0.1	0.1	5	0.50452099	2.91836987
			7							0.47473787	2.89627955
			10							0.43380880	2.86805053
0.5	0.01	0.5	5	0.1	3	1	0.1	0.1	5	0.50452099	2.91836987
				1						0.53356183	2.94334553
				5						0.59324405	2.99209859
0.5	0.01	0.5	5	0.1	3	1	0.1	0.1	5	0.50452099	2.91836987
					5					0.71398023	3.82159621
					7					0.83898353	4.55629077
0.5	0.01	0.5	5	0.1	3	1	0.1	0.1	5	0.50452099	2.91836987
						2				0.69054980	2.91497712
						3				0.76920997	2.91373875
0.5	0.01	0.5	5	0.1	3	1	0.1	0.1	5	0.50452099	2.91836987
							0.5			0.46611065	2.85048592
							1			0.40837695	2.79177067
0.5	0.01	0.5	5	0.1	3	1	0.1	0.1	5	0.50452099	2.91836987
								0.4		0.35177977	2.93714786
								0.7		0.26287285	2.93958487
0.5	0.01	0.5	5	0.1	3	1	0.1	0.1	5	0.50452099	2.91836987
									10	0.50247350	4.20518703
									15	0.50163494	5.18960129

Chapter 4

Conclusions and Future Scope

4.1 Conclusions drawn from Chapters

The research work presented in the current thesis provides a theoretical insight into the unsteady three dimensional flow of a couple stress Casson fluid in the presence of a magnetic field taking into account th effects of Hall current, thermal radiation, Newtonical heating at the surface. The thesis investigates the problem with or without the presence of the nano-particles. In chapter-2, the mass transfer aspect is also discussed whereas in chapter-3, the Brownian motion and thermopherotic diffusion effects are included to capture the implications of presence of nano-particles. The important findings of the thesis, drawn from chapter-2 and chapter-3, are summarized below:

1. The Casson parameter retards the fluid motion in x- and z-directions both. In case of the flow of a nanofluid, however, the effect is opposite near the surface of the sheet. The temperature of the fluid and species concentartion tend to rise due to an increase in the yiels stress. It tends to enhance the skin-friction in z-directions in both the cases.

2. In case of a clear fluid, the skin-friction coefficient increases and, in case of a nanofluid, the skin-friction coefficient decreases with increasing yield stress. The rate of heat and mass transfer increases with increasing Casson parameter.

3. Once again, the thermal radiation effects are prominently visible in case of a nanofluid flow. However, the observed effect is same. The thermal radiation increases the temperature of the fluid in the boundary layer region in both the

cases. In the later case, i.e, in case of nanofluid flow, the effect is more due to the presence of Brownian motion of the nano-particles. In both the cases, the rate of heat transfer decreases with increasing thermal radiation.

4.2 Scope for Future Research

While developing the mathematical model of physical problems, the low magnetic Reynolds number assumption is utilized to neglect the effects of induced magnetic field. Thus, one way of extending the work presented in the thesis is to relax the assumption and consider the effect of induced magnetic field. The work presented in this thesis may also be extended by applying similarity transformations which transform the governing non-linear partial differential equations into non-similar partial differential equations instead of non-linear ordinary differential equations.

Bibliography

[1] B.C.Sakiadis, Boundary layer behaviour on continous solid surfaces, A. I. Ch. E. Journal 7 (1961) 26–28.

[2] L. J. Crane, Fow past a stretching sheet, Zeit. Angew. Math. Mech 21 (1970) 6–45.

[3] P. Carragher, L. J. Crane, Flow and heat transfer on a stretching surface in a rotating fluid with a magnetic field, Zeit. Angew. Math. Mech 62 (1982) 5–64.

[4] P. S. Gupta, A. S. Gupta, Heat and mass transfer on a stretching sheet with suction or blowing, Can. J. Chem. Engng. 55 (1977) 7–44.

[5] K. B. Pavlov, Magnetohydrodynamic flow of a incompressible viscous fluid caused by deformation of a plane, US. RJ 4 (1974) 146–147.

[6] I. Pop, T. Y. Na, A note on mhd flow over a stretching permeable surface, Mech. Res. Commun. 25 (1998) 263–269.

[7] R. Ellhahi, A. Riaz, Analytical solutions for mhd flow in a third grade fluid with variable viscosity, Mathematical and Computer modeling 52 (2010) 1783–1789.

[8] K. Y. Rajagopal, A. S. Gupta, T. Y. Na, Flow of a viscoelastic fluid over a stretching sheet, Rheol. Acta 23 (1984) 213–215.

[9] R. K. Dash, K. N. Mehta, G. Jayaraman, Casson fluid flow in a pipe filled with a homogeneous porous medium, Eng. J. Sci. 36 (1996) 1145–1156.

[10] R. B. Bird, G. C. Dai, B. Yarusso, The rheology and flow of viscoplastic materials, Rev. Chem. Engg. 1 (1983) 1–83.

[11] A. G. Fredrickson, Principles and applications of rheology, NJ. USA. Prentice-Hall Englewood Cliffs.

[12] T. Hayat, S. A. Shehzadi, A. Alsaiedi, Soret and dufour effects on magnetohydrodynamic (mhd) flow of casson fluid, Appl. Math. Mech. Engl. Ed. 33 (2012) 1301–1312.

[13] R. C. Sharma, M. Sharma, Effect of suspended particles on couple stress fluid heated from below in the presence of rotation and magneticfield, Indian Journal of Pure and Apllied Mathematics 35 (2004) 973–989.

[14] D. Srinivasacharya, N. Srinivasacharyulu, O. Odelu, Flow and heat transfer of couple stress fluid in a porous channel with expanding and contracting walls, International Communications in Heat and Mass Transfer 36 (2009) 180–185.

[15] J. R. Lin, C. R. Hung, Combined effects of non-newtonian couple stresses and fluid inertia on the squeeze film characteristics between a long cylinder and an infinite plate, Fluid Dyn. Res. 39 (2007) 616–631.

[16] D. Pal, Hall current and mhd effects on heat transfer over an unsteady stretching permeable surface with thermal radiation, Compt. Math. Appld 66 (2013) 1161–1180.

[17] M. M. Bhatti, M. M. Rahidi, Study of heat and mass transfer with joule heating on magnetohydrodynamic(mhd) peristsltic blood flow under the influence of hall current, Propulsion and Power Research 6 (2017) 177–185.

[18] M. S. Ansari, R. Nandkeolyar, S. S. Motsa, P. Sibanda, Viscoelastic nanofluid flow and radiative nonlinear heat transfer over a stretching sheet, Journal of Computational and Theoretical Nanoscience 12 (2015) 1–10.

[19] B. Ganga, S. M. Y. Ansari, N. V. Ganesh, A. K. A. Hakeem, Mhd flow of boungiorno model nanofluid over a vertical plate with internal heat generation/absorption, Propulsion Power Research 5 (2016) 211–222.

[20] R. Biswas, S. F. Ahmmed, Effects of the hall current and chemical reaction on mhd unsteady heat and mass transfer 0f casson nanofluid through a vertical plate, J. Heat Transfer 140 (2018) 12.

[21] B. Mahanthesh, B. J. Gireesha, R. S. R. Gorla, Unsteady three-dimensional mhd flow of a nona eyring-powell fluid past a convectively heated stretching sheet in the presence of thermal radiation, viscous disssipation and joule heating, Journal of the Association of Arab Universities for Basic and Applied Sciences 23 (2017) 75–84.